THERMAL MANAGEMENT OF OUTSIDE PLANT TELECOMMUNICATION CABINETS: DESIGN AND CFD MODELING METHODOLOGY

by

FEROZ AHAMED IQBAL MARIAM

Presented to the Faculty of the Graduate School of

The University of Texas at Arlington in Partial Fulfillment

of the Requirements

for the Degree of

MASTER OF SCIENCE IN MECHANICAL ENGINEERING

THE UNIVERSITY OF TEXAS AT ARLINGTON

MAY 2010

ACKNOWLEDGEMENTS

I would like to thank my advisor, Prof. Dereje Agonafer, for the guidance and support he has provided. Without his experience and constant encouragement, the completion of this research work would have been very difficult.

I would also like to thank Prof. Haji-Sheikh and Prof. Nomura for serving on my committee. Additionally, I would like to express my gratitude to Mark Hendrix and Deepak Sivanandan for their industrial guidance and support during the course of this research.

Special mention needs to be given to Veerendra Mulay for his help and also Sally Thompson for her assistance in all matters. I would like to thank all my family and friends who have supported me and helped me through these years.

Finally, I would like to dedicate this work to my parents, Iqbal Ahamed and Mariam Beevi. For without their love and sacrifice I would not have been in a position to complete this work.

April 19, 2010

ABSTRACT

THERMAL MANAGEMENT OF OUTSIDE PLANT TELECOMMUNICATION CABINETS: DESIGN AND CFD MODELING METHODOLOGY

Feroz Ahamed Iqbal Mariam, M.S.

The University of Texas at Arlington, 2010

Supervising Professor: Dereje Agonafer

Over the years there has been a steady increase in the number of transistors being packed into the same footprint of a die, which has led to an increase in the power densities of electronics. The thermal management of electronic equipment therefore is becoming an integral part of packaging design.

Access networks provide the last mile of connectivity for the telecommunication network users. In the access network, the outside plant telecommunication cabinets houses electronic components and switching devices. These cabinets are standalone outdoor enclosures, and many a times they are located in hostile environments. Therefore, it is necessary that these cabinets provide environmental protection and thermal management for the electronics housed in it.

The first part of the thesis deals with the design and thermal analysis of air-cooled high powered telecommunication cabinets. Commercial CFD code has been used to design and compare various cabinet configurations. This has enabled in reducing the unnecessary

construction of cabinet prototypes and elaborate experimental tests, resulting in cost savings and reduction in lead time.

The electronics in these cabinets are powered by DC current and have backup batteries to support them in the event of a power failure. The life of a battery is dependent on the nature of the load applied, recharging conditions and most importantly ambient temperatures. Based on the location and time of day, the ambient temperature can be anywhere between -40℃ to 50℃. But for long standing battery life, the tempe rature inside the battery compartment should be maintained at 25℃. Active cooling using air-con ditioners are often used to achieve this, but air-conditioners are difficult to backup and are high in maintenance. A more convenient way to cool the battery compartments are to use Thermo-electric Coolers (TEC), as they are compact and quiet in operation. The second part of the thesis explains a modeling methodology to develop a TEC air-to-air heat exchanger that is used in the thermal management of the battery compartments. The numerical results thus obtained are validated with experimental results, and the validated model is further used to try out various test scenarios for the telecommunication cabinet.

TABLE OF CONTENTS

LIST OF ILLUSTRATIONS

LIST OF TABLES

NOMENCLATURE

ρ	Density (kg/m^3)
u	Velocity (m/s)
μ	Viscosity (N/m^2s)
p	Pressure (Pa)
B_x	Body force in the x-direction per unit volume (N/m^3)
V_x	Viscous force in the x-direction per unit volume (N/m^3)
h	Specific enthalpy (J/Kg)
k	Thermal conductivity (W/m-K)
T	Temperature (K)
S_h	Volumetric rate of heat generation (W/m^3)
G	Rate of generation of turbulence energy
ε	Kinematic rate of dissipation (m^2/s^3)
μ_t	Dynamic viscosity of the turbulent quantity (kg/m^2s)
σ_k	Constant for k - ε model (1.3)
Δp	Pressure drop (Pa)
f	Loss coefficient (m^{-1})
v	velocity (ms^{-1})
$\dot{Q}$	Rate of heat transfer (W/s)
$\dot{m}$	Mass flow rate (kg/s)
c_p	Specific heat (J/kg-K)
G	Volumetric flow rate (CFM)
N	Fan speed (RPM)

HP	Fan power (W)
α	Seebeck coefficient (V/℃)
i	Current (A)
K	Thermal conductivity of the thermoelectric material (W/m-K)
T_c	Cold side temperature (℃)
T_h	Hot side temperature (℃)
T_{amb}	Ambient temperature (℃)
Q_h	Heat delivered at the hot side of the TEC module (W)
Q_c	Heat pumped by the cold side of the TEC module (W)
Q_{TEC}	Heat generated by a TEC module (W)

CHAPTER 1

INTRODUCTION

1.1 Telecommunication Cabinets

Telecommunication cabinets are used to house electronic components like phone switches, optical fiber cables, transmitters and receivers. They are usually located close to the customer, remote from the central telecommunication office, and located in outdoor environments. This poses new challenges for packaging the electronics housed by these cabinets.

These enclosures need to protect these equipments from elements of nature like humidity, solar heating, dust, salt fog, electromagnetic interference and vandalism. They should also provide sufficient cooling or heating to the equipment depending on the ambient temperatures and the heat loads generated by the electronics.

The thermal management of telecommunication cabinets also called Outside Plant (OSP) cabinets comes under the category of system level packaging. With the increase in performance of the CMOS chip and the corresponding reduction in size, it has led to an increase in the heat density of the chips. This has given rise to the need for a more robust thermal management system at the device, board and system level packages that house these electronics.

Figure 1.1 is the graph by ASHRAE TC 9.9 which shows the increase in power density of IT equipments [1]. Electronic components typically have a temperature of 65℃ - 85℃ for commercial applications and from 110℃ - 125℃ for military applications. In addition to high temperatures, excessive temperature cycling can result in the reduction of life of the electronics. Therefore it is necessary to maintain relatively steady temperatures [2].

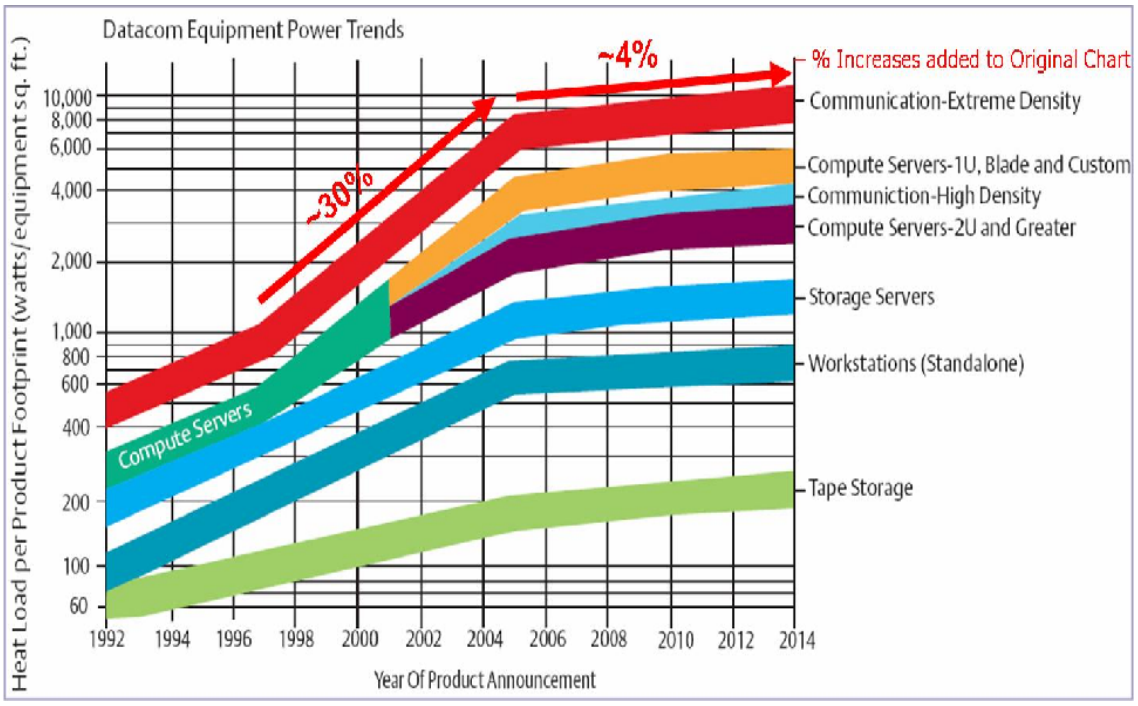

Figure 1.1 Heat load trends in electronics enclosures

1.2 Why Telecommunication Cabinets are Required?

Outdoor telecommunication cabinets are found in the 'last mile' of the telecommunication access network. They provide support for both wireless and wire-line applications. They are used as Optical Network Terminals or Units (ONT or ONU).

Optical access networks enable carriers to offer any kind of service over a single network [3]:

- Multiple voice channels using voice over IP.
- Multiple qualities of service data offering.
- Video offered either in an overlay configuration or within the data stream.

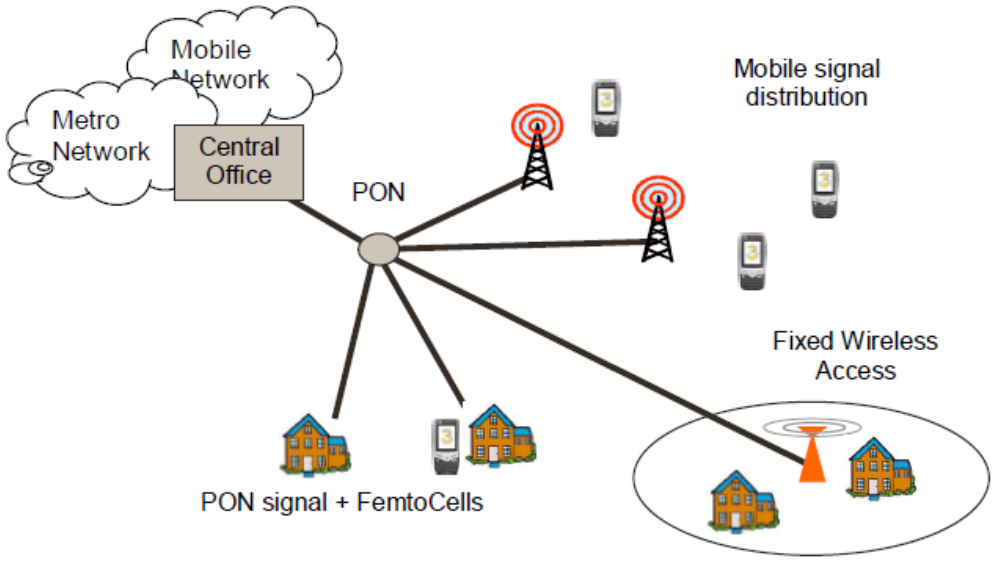

Figure 1.2 Metropolitan FTTX access network

Access bandwidth demand is constantly increasing due to the arrival of new applications such as HDTV, P2P applications, video on demand, interactive games, e-learning and the use multiple PCs at home. As a result, residential users may require connections of more than 1 Gb/s.

Common access architecture is the Fiber to the x (FTTX) where X stands for premise, home, business etc. There are two alternative solutions within FTTX to introduce optical fiber in the access loop: Point-to-point (PTP) and Point-to-multipoint (PTMT). PTP is used mostly used for business services, as it provides higher bandwidth, and PTMT is used mostly for residential applications. Figure 1.2 shows a typical metropolitan FTTX access network [4].

1.3 Computational Fluid Dynamics Analysis of Telecommunication Cabinets

Computational Fluid Dynamics tools help system designers to drastically reduce the time-to-market for products. Over the past decade there has been a drastic increase in the use of CFD tools in the design and development of electronics at the device level, systems level and the data center level. Interest in thermal simulations is driven by the need to understand the

performance and reliability impacts of the operating conditions and the environments. These simulations also play a central role in the selection and sizing of thermal management solutions.

The accuracy of the numerical model depends on a number of factors. First is the type of algorithm used. The algorithm can be a finite element or finite volume one, it could use structured or unstructured mesh and the method of discretization. Second is the mesh size and time steps employed. A grid refinement effort should be made to ensure that the results are independent of the grid size and time step. Thirdly is the treatment of multimode effects, conduction and convection play an important role in system level packages. In some cases involving cooling by natural convection, radiation also plays an important role and is comparable to convection [5]. In such cases, the inclusion of radiation in the modeling also becomes important.

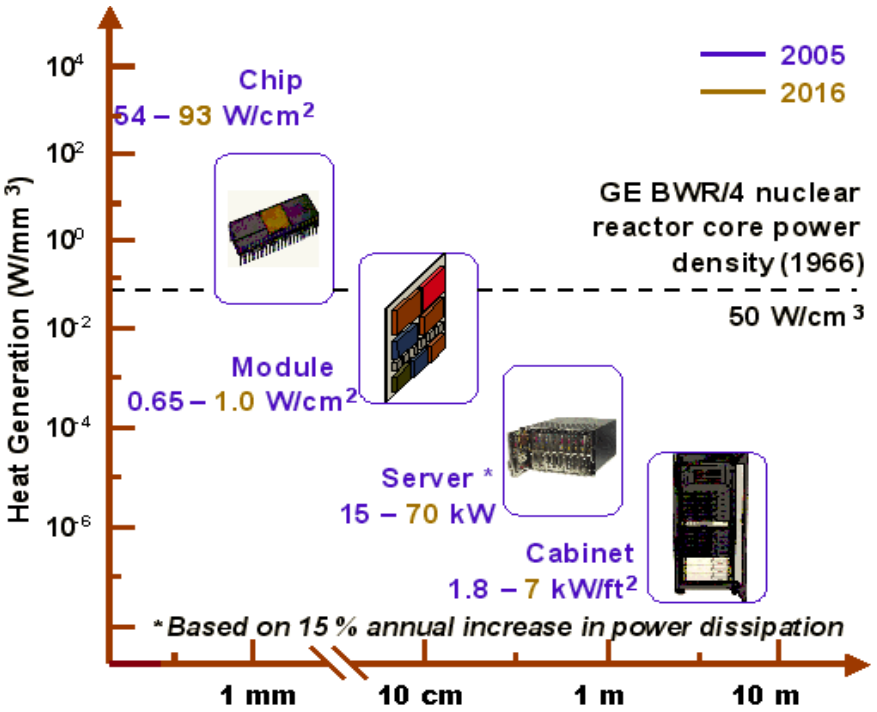

Figure 1.3 Hierarchy of package length scales and their typical heat generation rate

Numerical modeling of telecommunication cabinets involves a hierarchy of length scales, ranging from 10^{-4} m to 1 m. Figure 1.3 shows a 'chip-to-cabinet' variation in length scales involved [6]. The use of devices like heat sinks and fans result in complex local flow patterns that are difficult to resolve with grid sizes selected for the entire system. The use of localized meshing or conformal meshing is required to mitigate this problem.

1.4 Telecommunication Cabinets Industry Standards

The telecommunication industry has enforced standards to ensure that cabinet manufactures meet certain performance and safety requirements for their products. Further, these standards specify how and for what these equipments are to be tested. Some of the important standards for cabinets in North America are NEMA ratings, Telcordia GR-CORE standards and the Underwriters Laboratory (UL) standards.

1.4.1 National Electrical Manufacturers Association (NEMA) Standards

The specific enclosure types, their applications and their environmental conditions are designed to protect against are specified by the NEMA standards [7]. For non-hazardous locations there are 16 classifications of enclosures out of these 10 of them are commonly followed by telecommunication standards for outside plant cabinets. They are listed below:

Type 3 - Enclosures constructed for either indoor or outdoor use to provide a degree of protection to personnel against access to hazardous parts; to provide a degree of protection of the equipment inside the enclosure against ingress of solid foreign objects (falling dirt and windblown dust); to provide a degree of protection with respect to harmful effects on the equipment due to the ingress of water (rain, sleet, snow); and that will be undamaged by the external formation of ice on the enclosure.

Type 3R - Enclosures constructed for either indoor or outdoor use to provide a degree of protection to personnel against access to hazardous parts; to provide a degree of protection of the equipment inside the enclosure against ingress of solid foreign objects (falling dirt); to provide a degree of protection with respect to harmful effects on the equipment due to

the ingress of water (rain, sleet, snow); and that will be undamaged by the external formation of ice on the enclosure.

Type 3S - Enclosures constructed for either indoor or outdoor use to provide a degree of protection to personnel against access to hazardous parts; to provide a degree of protection of the equipment inside the enclosure against ingress of solid foreign objects (falling dirt and windblown dust); to provide a degree of protection with respect to harmful effects on the equipment due to the ingress of water (rain, sleet, snow); and for which the external mechanism(s) remain operable when ice laden.

Type 3X - Enclosures constructed for either indoor or outdoor use to provide a degree of protection to personnel against access to hazardous parts; to provide a degree of protection of the equipment inside the enclosure against ingress of solid foreign objects (falling dirt and windblown dust); to provide a degree of protection with respect to harmful effects on the equipment due to the ingress of water (rain, sleet, snow); that provides an additional level of protection against corrosion and that will be undamaged by the external formation of ice on the enclosure.

Type 3RX - Enclosures constructed for either indoor or outdoor use to provide a degree of protection to personnel against access to hazardous parts; to provide a degree of protection of the equipment inside the enclosure against ingress of solid foreign objects (falling dirt); to provide a degree of protection with respect to harmful effects on the equipment due to the ingress of water (rain, sleet, snow); that will be undamaged by the external formation of ice on the enclosure that provides an additional level of protection against corrosion; and that will be undamaged by the external formation of ice on the enclosure.

Type 3SX - Enclosures constructed for either indoor or outdoor use to provide a degree of protection to personnel against access to hazardous parts; to provide a degree of protection of the equipment inside the enclosure against ingress of solid foreign objects (falling dirt and windblown dust); to provide a degree of protection with respect to harmful effects on the

equipment due to the ingress of water (rain, sleet, snow); that provides an additional level of protection against corrosion; and for which the external mechanism(s) remain operable when ice laden.

Type 4 - Enclosures constructed for either indoor or outdoor use to provide a degree of protection to personnel against access to hazardous parts; to provide a degree of protection of the equipment inside the enclosure against ingress of solid foreign objects (falling dirt and windblown dust); to provide a degree of protection with respect to harmful effects on the equipment due to the ingress of water (rain, sleet, snow, splashing water, and hose directed water); and that will be undamaged by the external formation of ice on the enclosure.

Type 4X - Enclosures constructed for either indoor or outdoor use to provide a degree of protection to personnel against access to hazardous parts; to provide a degree of protection of the equipment inside the enclosure against ingress of solid foreign objects (windblown dust); to provide a degree of protection with respect to harmful effects on the equipment due to the ingress of water (rain, sleet, snow, splashing water, and hose directed water); that provides an additional level of protection against corrosion; and that will be undamaged by the external formation of ice on the enclosure.

Type 5 - Enclosures constructed for indoor use to provide a degree of protection to personnel against access to hazardous parts; to provide a degree of protection of the equipment inside the enclosure against ingress of solid foreign objects (falling dirt and settling airborne dust, lint, fibers, and filings); and to provide a degree of protection with respect to harmful effects on the equipment due to the ingress of water (dripping and light splashing).

Table 1.1 Comparison of Applications of Enclosures for Outdoor Non-hazardous Locations

Provides a Degree of Protection Against the Following Conditions	**Type of Enclosure**									
	3	**3X**	**3R***	**3RX***	**3S**	**3SX**	**4**	**4X**	**6**	**6P**
Access to hazardous parts	X	X	X	X	X	X	X	X	X	X
Ingress of water (Rain, snow, and sleet ****)**	X	X	X	X	X	X	X	X	X	X
Sleet *****	...	...	...	...	X	X	...	...	...	...
Ingress of solid foreign objects (Windblown dust, lint, fibers, and flyings)	X	X	...	...	X	X	X	X	X	X
Ingress of water (Hosedown)	...	...	...	...	...	...	X	X	X	X
Corrosive agents	...	X	...	X	...	X	...	X	...	X
Ingress of water (Occasional temporary submersion)	...	...	...	...	...	...	...	...	X	X
Ingress of water (Occasional prolonged submersion)	...	...	...	...	...	...	...	...	...	X

* These enclosures may be ventilated.
** External operating mechanisms are not required to be operable when the enclosure is ice covered.
*** External operating mechanisms are operable when the enclosure is ice covered.

Type 6 - Enclosures constructed for either indoor or outdoor use to provide a degree of protection to personnel against access to hazardous parts; to provide a degree of protection of the equipment inside the enclosure against ingress of solid foreign objects (falling dirt); to provide a degree of protection with respect to harmful effects on the equipment due to the ingress of water (hose directed water and the entry of water during occasional temporary submersion at a limited depth); and that will be undamaged by the external formation of ice on the enclosure.

Type 6P - Enclosures constructed for either indoor or outdoor use to provide a degree of protection to personnel against access to hazardous parts; to provide a degree of protection of the equipment inside the enclosure against ingress of solid foreign objects (falling dirt); to provide a degree of protection with respect to harmful effects on the equipment due to the ingress of water (hose directed water and the entry of water during prolonged submersion at

a limited depth); that provides an additional level of protection against corrosion and that will be undamaged by the external formation of ice on the enclosure.

Table 1.1 shows the specific application of different type of enclosures for outdoor non-hazardous locations.

1.4.2 Telcordia GR Standards

The Telcordia Generic requirements(GR) is used by telecommunication cabinet manufactures to design or test their equipment. There are generally three standards that are commonly followed for outdoor telecommunication cabinets. They are Telcordia GR-63, GR-487 and GR-1089 [8].

Telcordia GR-63 - This Generic Requirements document (GR) presents minimum spatial and environmental criteria for all new telecommunications equipment used in Central Offices (COs) and other environmentally controlled telephone equipment spaces. These NEBS (Network Equipment-Building System) criteria were developed jointly by Telcordia and industry representatives. They are applicable to switching and transport systems, associated cable distribution systems, distributing and interconnecting frames, power equipment, operations support systems, and cable entrance facilities

Telecommunications equipment, by nature of its physical installation in a building, may be exposed to environmental stresses. The NEBS generic criteria are intended to help avoid equipment damage and malfunction caused by such things as temperature and humidity, vibrations, airborne contaminants, minimize fire ignitions and fire spread, as well as provide for improved space planning and simplified equipment installation.

Telcordia GR-487 - This requirement provides criteria for analyzing Electronic Equipment Cabinets used in a variety of outside plant environments and applications, including wireless. It includes proposed functional design criteria, generic mechanical and environmental requirements, desired features,

and performance tests. It covers cabinet requirements on thermal test procedure, acoustic noise issues, environmental vibration criteria and Restriction of Hazardous Substance(RoHS) criteria.

Telcordia GR-1089 - Telecommunications service providers have used GR-1089 to ensure their telecommunications equipment contained the Electromagnetic Compatibility (EMC) and electrical safety criteria necessary to perform safely and reliably. The NEBS (Network Equipment-Building System) criteria in this reference covers equipment in central offices; equipment in the outside plant at locations such as controlled environmental vaults, electronic equipment enclosures, and huts; equipment in uncontrolled structures such as cabinets; and network equipment at the customer premises.

Telecommunications equipment, by nature of its application in the telecommunications network, may be exposed to one or more sources of electromagnetic energy. The system-level generic criteria for EMC in this standard are intended to help avoid equipment damage and malfunction because of lightning, 60-Hz commercial power fault conditions, Electrostatic Discharge (ESD), Electrical Fast Transient (EFT), Electromagnetic Interference (EMI), operation in the presence of a dc potential difference, and operation in a steady-state induced voltage environment.

1.4.3 Underwriters Laboratory (UL) Standards

The most commonly used Underwriters Laboratory standard in the outdoor telecommunication cabinet industry is the UL-50 standard. This standard covers the non-environmental construction and performance requirements for enclosures to provide a degree of protection to personnel against incidental contact with the enclosed equipment [9].

CHAPTER 2

LITERATURE REVIEW

There has been considerable research in the field of thermal management of outside plant telecommunication cabinets. There are numerous papers which details different cooling technologies for the cabinets. Also considerable research has gone into the development of numerical and analytical modeling methodologies for these cabinets. Some of these previous research work have been summarized in this chapter and are as follows:

1. Cooling technologies
2. Modeling methodologies

2.1 Cooling Technologies

2.1.1 Natural Convection

Maringou et al. in [10] discusses the design of an outdoor enclosure that cools the electronics passively. Two passive cooling methods are discussed, natural convection and phase change materials (PCM). The former is chosen due to space restrictions as a PCM based cooling system could not be accommodated. The cabinet is designed to house fairly low power electronics and a study is done to compare the temperature inside the cabinets, with and without solar loading. It was found that without solar heating the temperature just crossed the design mark by 2-3℃. So the cooling system had to account for the temperature rise due to the electronics as well as the solar heating. A double-finned air-to-air heat sink was developed. This heat sink took the shape of long plate fins on either side of the solid wall of the cabinet. The outer side of the cabinet was shrouded to shield it from the solar heating. The design was developed numerically using CFD code ICEPAK and experimentally tested using simulated solar loads in a temperature controlled chamber to corroborate the CFD results.

In the experimental setup, Garcia et al [11] uses a square box to simulate a telecommunication cabinet, which used trapezoidal channels to enhance natural convection of heat from the cabinet. The wall consisted of thin aluminum sheets between which a triangular corrugated sheet was placed. The enclosure was tested with horizontal and vertical channels and also without channels to set the benchmark case. Transient heat analysis was performed. The numerical analysis was done using Flotherm, and the results were validated with the experimental results. Through these tests it was observed that addition of channels substantially affected the temperature inside the cabinet. The addition of vertical or horizontal channels enhances heat transfer at low heat loads i.e. at low Rayleigh numbers. But as the heat loads increases (higher Rayleigh numbers) the effectiveness of the channels decreases.

In order to predict the total heat transfer rate, an analytical based model was developed by Teerstra et. al.[12]. The system consists of an isothermal plate in an isothermal cuboid enclosure. A model that is valid over a wide range of enclosure/plate geometries and flow conditions were developed. The authors combined three asymptotic solutions: pure conduction through the enclosed region, laminar boundary layer flow and transition flow convection into a composite expression.

The model requires no correlation coefficients and is not limited to a certain range of values of the independent parameters. The analytical model was validated with numerical data from two CFD codes, ICEPAK and Flotherm , and the agreement between the analytical and numerical results was within 10%.

2.1.2 Phase Change Materials (PCM)

Porebski et al [13] discusses the development of a thermal battery which houses PCM materials. This thermal battery can be used effectively in relatively small enclosures. In this paper he explains the energy balance equation to calculate the mass of PCM that is required for the system. They test three different PCM materials to come out with the best one. Through the experimental setup it was determined that the use of PCM based thermal battery is effective during peak loads. Also improved temperature stabilization was observed with PCM thermal battery wherever there was a swing in the ambient temperature.

In [14] Maringiu explains the development of cooling technology that is a combination of PCM heat exchangers with active air movers and channeled walls which act as solar load mitigations. The PCM material is encapsulated in tubes which are arranged in aligned or staggered bundles. During daytime the warm air is blown over the PCM containing tubes by the fan and during night time, the cool night air flows over the tubes to change the material back to the liquid phase.

The PCM heat exchanger was numerically modeled using the CFD software, FIDAP. Glauber's salt was used as the phase changing material. It was found that the channeled wall took care of the solar loading and the thermal management of the cabinet was attained with the PCM heat exchanger. Four different channel configurations were tested: parallel plate, triangular, circular and square. It was found that the circular configurations gave the best results.

Consentino [15] explains the use of PCM as a passive means to cool the battery compartments of outdoor telecommunication cabinets. The PCM was in the form of a solid vinyl jacket which was strapped around the batteries. The PCM material chosen was commercially called TEAP 29. The testing was done for four weeks in the temperate climate of Chicago. It was observed that the peak excursions were greatly reduced as compared to a control cabinet which had no PCM jackets for its batteries. In the second phase of the test the PCM jacket

design was changed to PVC jacket so that it could be aligned vertically to take advantage of gravity to assist natural convection. The new jacket configuration was tested in an environmental chamber to day/night cycle. The standard deviation of the control battery was 3.5ºC and the battery with the PCM jacket was 1.6ºC.

2.1.3 Heat Exchangers

In [16], Choi et al the performance of a hybrid refrigeration cooling system for telecommunication equipment was analyzed and measured for various operating conditions. The test setup consisted of a unit rack of the telecommunication equipment. It consisted of PCB board, fans and a fin plate heat exchanger. The hybrid cooling system had two modes of operation, for high outdoor temperature the system operates in the vapor compression mode and for low outdoor temperatures operates in the secondary cooling mode, with no operation of the compressor. Because of this dual mode of operation, the COP of the hybrid refrigeration system was significantly enhanced for low outdoor temperature due to no operation of the compressor.

Marongiu [17] discusses a compact heat exchanger made of heat pipes that is used to cool the battery compartment of an outdoor telecommunication cabinet. The heat exchanger has a high efficiency because its transfer surfaces are made of heat pipes. The heat exchanger consists of two parts, the bottom part is located in the battery compartment and the top part is located in the electronics compartment which is cooled by an air-conditioning system. The heat pipes transfer heat from the bottom compartment into the top electronic compartment, where cold air from the air conditioner forms the cold loop of the heat exchanger. Performance analysis was done analytically using standard empirical data. Results of a parametric study showed that the heat exchanger can remove up to 250 W of heat for an air conditioner supply temperature of 20ºC.

2.1.4 Double Walled Cabinets

In [18] Muralidharan et al discusses the impact of a double wall in the thermal management of an outside plant telecommunication cabinet. Different types of double wall configuration has been considered and numerically tested. The CFD code used is Flotherm. Three configurations with double wall on the sides of the cabinet, double wall on the sides and top and double wall with forced circulation using fans have been discussed. All these cases have been compared with a baseline case with no double walls. It was found that the double wall with forced convection returned the best results. It was also observed by the author that by varying the air gap from 1" to 3.5", no significant temperature reduction inside the cabinet was achieved.

Muralidharan et al [19] further investigates the different fan locations to minimize the energy consumption of the fans in a double wall configuration. Two fan locations were studied, first one had the top side of the double wall and the second one had fans at the bottom of the side walls. The gap of the walls also varied from 2" to 3". It was observed that having fans at the top provided the best results in terms of best temperatures as well as energy minimization.

2.2 Modeling Methodologies

2.2.1 Compact Modeling

One of the first compact models were developed by Linton and Agonafer [20], where they developed a coarse finned heat sink which can be used in system level modeling. The mesh size of the heat sink was reduced to 3x4x3 cells. Comparing it with experimental data the approximation error was within 18%.

Further improved compact models were later developed by Narasimhan and Bar-Cohen[21] by using a porous medium model. Comparing with a detailed model the agreement of the porous medium model was within 11% for pressure drop and 17.2% for base temperature predictions.

A dynamic compact model for an insulated gate bipolar transistor (IGBT) was created by Luo[22] by using experimental measurements. The experimental transient thermal impedance was fitted into a series that consisted of a finite number of exponential terms. The thermal circuit for the IGBT was created based on these terms. A detailed numerical model was created in Ansys and the compact model had predicted transient thermal impedance with a closeness of 11% with the detailed model.

Aalok et al in [23] has used the commercial CFD code Flotherm to numerically model a compact counter flow heat exchanger. The heat exchanger consists of 75 vertical fins between which the heat transfer between the hot and cold loop takes place. Since modeling such a geometry in detail would lead to a fairly large increase in the overall mesh count, the author uses the numerical capabilities of the software to model a compact heat exchanger.

'Volume source' which is an in-built macro in Flotherm is used to build the heat exchanger. The amount of heat absorbed or rejected is specified in this macro. Cooling capabilities of the heat exchanger is found by modeling the detailed heat exchanger in a simulated wind tunnel. The results of the detailed heat exchanger, compact heat exchanger and the test data are compared and show a closeness of less than 10%. Also, by using the compact model the author has achieved a mesh reduction of 45%.

2.2.2 Transient Modeling

McKay [24] developed an analytical transient model of a telecommunication cabinet. The model consisted of a single lumped thermal mass for the cabinet with a thermal resistance between the ambient air and the front and back side of the cabinet. The effect of solar loading on the cabinet was also considered. The results of the analytical model were compared with experimental test results.

CHAPTER 3

COMPUTATIONAL FLUID DYNAMICS (CFD) MODELING

CFD is concerned with the numerical simulation of fluid flow, heat transfer and chemical reactions. A numerical prediction works out the consequence of a mathematical model, which represents our physical domain of interest that needs to be analyzed. In this study, it involves the system level electronics like the telecommunication cabinets, the equipment housed by the cabinet, the surrounding conditions like the ambient temperature, solar heat load and wind flow.

3.1 The Governing Differential Equations

The numerical solution for heat transfer and fluid flow based problems is obtained from solving a series of three differential equations, called the Governing Differential equations. They are the conservation of mass, conservation of momentum and conservation of energy [25].

For a generalized case the conservation of mass is given by:

$$\frac{\partial \rho}{\partial x} + div(\rho u) = 0 \tag{3.1}$$

The conservation of momentum for a generalized case is given by:

$$\frac{\partial}{\partial t}(\rho u) + div(\rho u u) = div(\mu \, grad \, u) - \frac{\partial p}{\partial x} + B_x + V_x \tag{3.2}$$

The conservation of Energy for a steady low velocity flow is given by:

$$div(\rho u h) = div(k \, grad \, T) + S_h \tag{3.3}$$

3.2 Computational Domain or Domain of Integration

The region of space in which the governing differential equations are to be solved is called the computational domain (domain of integration or solution domain). The solutions to the governing equations are obtained by setting the boundary condition for the solution domain.

These boundary conditions for the study of outdoor cabinets include, but are not limited to, the ambient temperature, free stream velocity and solar radiation. The conditions of the domain wall faces also needs to be considered in the problem i.e. whether they are open, no-slip or symmetric. Also, as part of the problem formulation the properties of the fluid like its conductivity, density, viscosity, specific heat, expansivity and diffusivity needs to be specified [26].

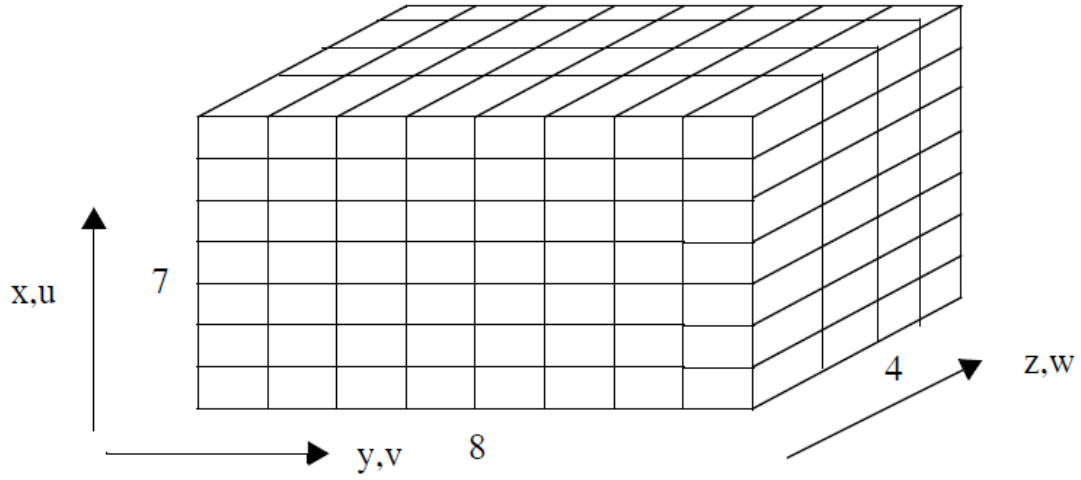

Figure 3.1 Graphical representation of a 3D grid

The governing equations and their associated boundary conditions do not have a general analytical solution. There are particular solutions for simple problems like a laminar flow in a rectangular channel. But for complex and more real world problems, the equations can only be solved numerically. The CFD code used for this study, Flotherm, is based on the Finite Volume Method (FVM). The first step in an FVM is to discretize the solution domain into a number of control volumes or grid cells, where the variables to be calculated is located at the centroid of the finite volume. The graphical representation of grids or elements is shown in Figure 3.1.

FVM works by integrating the differential form of the governing equations over each control volume. The Finite Volume Method has the advantage that it satisfies the conservation

of quantities like mass, momentum and energy. This is observed in any control volume and also over the entire computational domain.

The discretization results in a set of algebraic equations, each of which relates the value of a variable in a cell to its value in the nearest neighbor cell. Taking the example of T, the temperature variable, it is computed by the algebraic equation:

$$T = \frac{C_0T_0 + C_1T_1 + C_2T_2 + C_3T_3 + C_4T_4 + C_5T_5 + C_6T_6 + S}{C_0 + C_1 + C_2 + C_3 + C_4 + C_5 + C_6} \quad (3.4)$$

Where T1, T2, T3, T4, T5, T6 are the temperature values in the six neighboring cells and T0 is the value in the old time step. The Cs denotes the coefficient that connects the in-cell value to each of its neighboring cell values and S denotes the source term. If there are n cells in the solution domain there are a total of 5n algebraic equations to solve. This is because there are algebraic equations to solve for each field variables T, u, v, w, p.

The above expression is in reality a non-linear equation as the coefficients are also a function of T, u, v, w, p. But its appearance of linearity can be exploited to compute the value iteratively. For each outer iteration, the coefficients are calculated once and then taken as constant and the resulting algebraic equations are solved by means of inner iterations.

Normally more grid is used in regions of the domain where the gradients of the variable are expected to be the highest. Finer the grid better the algebraic equations approximates to the governing differential equations. It should be noted that having a grid independent solution alone does not guarantee a solution that simulates close to the real world problem. Other factors like the accuracy of the boundary conditions, the adequacy of the turbulence model affect the outcome of the solution and its closeness to reality.

3.3 Turbulence Modeling

The most prevalent method for cooling electronics is air-cooling. The air-flow regime in electronics usually ranges from laminar flow to the low Reynolds number turbulent flow. The two common ways by which Flotherm models this low Reynolds number turbulence flow region is by the LVEL turbulence model and the K-Epsilon turbulence model.

3.3.1 LVEL Turbulence Model

The LVEL turbulence model, also called the automatic algebraic method, is an algebraic model which removes the need for any user-defined velocity or length scale. This model requires the distance to the nearest wall (L) the local velocity (VEL) and the laminar viscosity. It has the advantage of being computationally inexpensive and can be easily applied to three dimensional problems.

The maximum local length scale and the distance to the nearest wall can be computed from the following equations:

$$D = \sqrt{|\nabla\varphi|^2 + 2\varphi} \tag{3.5}$$

$$L = D - |\nabla\varphi| \tag{3.6}$$

Where: $\nabla^2\varphi = -1$ with $\varphi = 0$ at the wall.

These length and velocity scales are computed for each cell and are used in conjunction with classical boundary layer wall functions to determine the turbulent viscosities for each cell [27]. Where Φ is the dependent variable.

The LVEL turbulence model provides a good prediction of the turbulence viscosities for cells near the walls, but provides unrealistically high turbulent viscosities in the free stream [28]. Therefore, this method of turbulence modeling is suited for electronics equipment like telecommunication cabinets, which has a high density of electronics that are close to each other and to the walls of the enclosure.

3.3.2 K-Epsilon Turbulence Model

The K-Epsilon model is a two equation model that is extensively used for turbulent fluid dynamics. This model computes viscosity on a grid cell to grid cell basis rather than computing viscosity as it is affected by the walls. It consists of two transport equations, one equation to describe the kinetic energy of turbulence and the second equation to represent the rate of turbulent dissipation [29].

The transport equations are:

$$\frac{\partial(\rho k)}{\partial t} + \frac{\partial(\rho k u_i)}{\partial x_i} = \frac{\partial}{\partial x_i}\left[\left(\mu + \frac{\mu_t}{\sigma_k}\right)\frac{\partial k}{\partial x_i}\right] + G_k + G_b - \rho\varepsilon \tag{3.7}$$

$$\frac{\partial(\rho\varepsilon)}{\partial t} + \frac{\partial(\rho\varepsilon u_i)}{\partial x_i} = \frac{\partial}{\partial x_i}\left[\left(\mu + \frac{\mu_t}{\sigma_k}\right)\frac{\partial \varepsilon}{\partial x_i}\right] + C_{1\varepsilon}\frac{\varepsilon}{k}(G_k + C_{3\varepsilon}G_b) - C_{2\varepsilon}\rho\frac{\varepsilon^2}{k} \tag{3.8}$$

The model is suited for dealing with problems with thin shear layers and recirculating flows. It is preferable to use this turbulence model for enclosures and rooms with large free-streams like datacenters and telecommunication shelters.

CHAPTER 4

TELECOMMUNICATION CABINET COMPONENTS

This chapter details the different telecommunication cabinet components that have been used for thermal and air-flow management in this study. The components are filters, fans and thermo-electric coolers. The selection criteria for these components in the design process has been explained. Also, the aspects of modeling these components using the commercial code Flotherm has also been touched upon.

4.1 Filters

Apart from the obvious reasons of removing dust and particulate contaminants, filters are used in telecommunication shelters to remove humidity, straighten air flow and also attenuate electromagnetic interferences (EMI). Filter selection is an important step in the cabinet design as the wrong filter can compromise the electrical and thermal performance of the electronics housed by it.

Particulate components removed by air filters can range from leaves and dust to more corrosive substances like solvents and salt fog. Solvents can cause corrosive damage to the electronics other particulate contaminants can accumulate in between electronics and cause electrical shorts and shrouding. This could lead to improper thermal management of the equipment causing its failure.

Hydrophobic filters are used to remove humidity from the air that enters the cabinet. They are provided with a membrane which absorbs water particles in the inlet stream of air.

Electromagnetic interference can cause malfunction or breakdown of some of the components housed by the cabinets. Metallic enclosures or cabinets by themselves provide adequate EMI protection but the presence of openings in the cabinet can allow electromagnetic or radio frequency interference to pass through. EMI filters are provided at these openings to

attenuate EMI. They often consist of a honeycomb mesh made out of aluminum and is often grounded. These honeycomb patterns are designed to reflect and absorb EMI noise.

Filters are also used to straighten air flow inside a system as less turbulent airflow is better from a fan efficiency point of view. Less turbulence means less friction and therefore less work done by the fan.

Table 4.1 Standards for Air-Filters

ASHRAE STD 52-76 synthetic dust weight arrestance	Measures the weight of test dust retained by the filter as a percentage of the total weight of dust used.
ASHRAE dust spot efficiency	Compares the discoloration effect of filtered air containing normal dirt particles with that of non-filtered air.
MIL-STD-282 DOP	Measures the percentage of Di-Octyl Phthalate smoke retained by the filter. The particle tested is 0.3 microns.

The two main operating characteristics of a filter are its filter efficiency and pressure drop. Filter efficiency is the percentage measure of the air borne particulates that a filter is able to remove from the flow at a given velocity. Standards to measure filter efficiency are given in Table 4.1[30].

Filter pressure drop is a measure of the force required to move air through the filter at a given velocity. The system resistance is the sum of all the pressure drops in the system and this includes the pressure drop across the filter. The air filter pressure drop is a function of the velocity of the air and the filter medium. Each filter medium will have a unique pressure versus air velocity characteristics, this is given by the filter performance curves, shown in Figure 4.1.

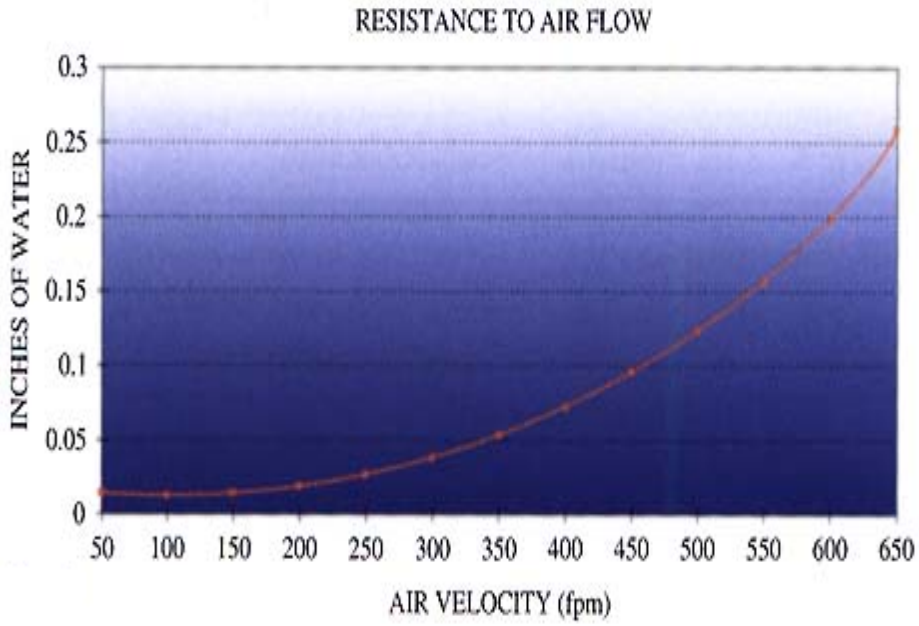

Figure 4.1 A typical air-flow filter resistance curve

For numerical modeling in Flotherm the filters are modeled using resistances. Resistances can be either planar or volume resistances. By modeling resistances, the effect of pressure drop and change in velocity similar to that of a filter can be incorporated in the model. This is attained by entering the loss coefficient and free-area ratio for the filter. The pressure drop is computed by:

$$\Delta p = \left(\frac{f}{2}\right) \times \rho \times v^2 \tag{4.1}$$

4.2 Fans

Fans are low pressure air pumps. They convert the torque supplied to the propeller to increase the static pressure across the fan rotor and also increase the kinetic energy of the air particles.

There are two types of fans that are commonly used in electronics cooling applications: axial flow fans and centrifugal blowers. Axial flow fans delivers air in the direction parallel to the fan blade axis and can be designed to deliver high flow rates. Blowers delivers air in the direction perpendicular to the blower axis and is usually designed to work against high pressure, but deliver relatively low flow rates.

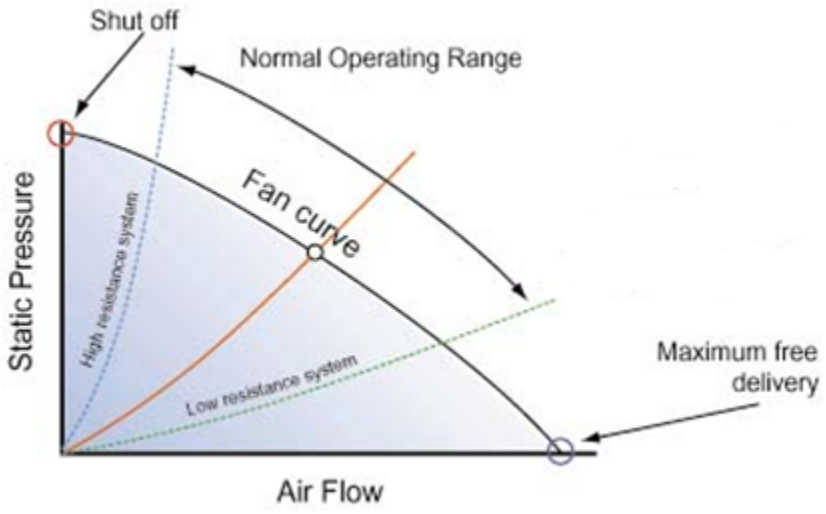

Figure 4.2 Typical fan performance curve

The aerodynamic characteristics of a fan are displayed in a fan performance curve. These curves show the relationship between volume flow rate and the pressure generated at various flow rates. The maximum flow rate is achieved at the free delivery condition and it represents the condition of maximum kinetic energy. The shut off point represents the condition of maximum potential energy, at this point the flow rate comes down to zero. Fan curves are very crucial for the selection of fans for cooling of a particular system. The

governing principle in fan selection is that any given fan can deliver only one flow at one pressure in a particular system. The intersection of the fan performance curve and the system impedance curve gives the operating point of that fan for that particular system. The figure 4.2 shows the operating point for both a high and low resistance system. From the point of view of a system designer it is better to select a fan that gives an operating point towards the high flow, low pressure end of the performance curve. This enables the fans to maintain higher propeller efficiency and avoid propeller stall [31].

For the selection of a fan it is necessary to have an estimate of the airflow that is required. This is obtained by using the basic heat transfer equation given by:

$$\dot{Q} = \dot{m} c_p \Delta T \tag{4.2}$$

$$\dot{m} = \rho G \tag{4.3}$$

A better prediction of the required airflow can be obtained by calculating the operating point using the airflow network analysis or using computational fluid dynamics software [32].

4.2.1 Fan Laws

Fan laws can be used to predict the fan performance at a second condition.

The fan law equations are:

$$G_2 = \frac{N_2}{N_1} \times G_1 \tag{4.4}$$

$$P_2 = \left(\frac{N_2}{N_1}\right)^2 \times P_1 \tag{4.5}$$

$$HP_2 = \left(\frac{N_2}{N_1}\right)^3 \times HP_1 \tag{4.6}$$

The commercial CFD code Flotherm, used in this study, allows the modeling of fans using the fan smart part. A 2D rectangular fan or a 3D axial flow fan can be modeled with this smart part. The code allows the user to input a fixed value for the flow rate as well as a fan curve for more precise modeling of systems.

4.3 Thermoelectric Coolers

Thermoelectric coolers (TEC) are solid state heat pumps used in applications where temperature stabilization, temperature cycling, or cooling below ambient are required. There are many products using thermoelectric coolers, including CCD cameras (charge coupled device), laser diodes, microprocessors, blood analyzers and portable picnic coolers. This article discusses the theory behind the thermoelectric cooler, along with the thermal and electrical parameters involved.

Thermoelectrics are based on the Peltier Effect, discovered in 1834, by which DC current applied across two dissimilar materials causes a temperature differential. Solid-state cooling such as thermoelectric or thermal diode is extremely important to future electronics thermal management because besides vapor compression and cryogenic, solid-state cooling is the only well-researched alternative technology that can achieve sub ambient cooling [33].

The typical thermoelectric module is manufactured using two thin ceramic wafers with a series of P and N doped bismuth-telluride semiconductor material sandwiched between them. The ceramic material on both sides of the thermoelectric adds rigidity and provides electrical insulation. The N type material has an excess of electrons, while the P type material has a deficit of electrons. One P and one N semiconductor make up a thermoelectric couple. The thermoelectric couples are electrically in series and thermally in parallel. A thermoelectric module can contain one to several hundred couples [34]. Figure 4.3 shows the internal structure of a TEC with the P and N junctions.

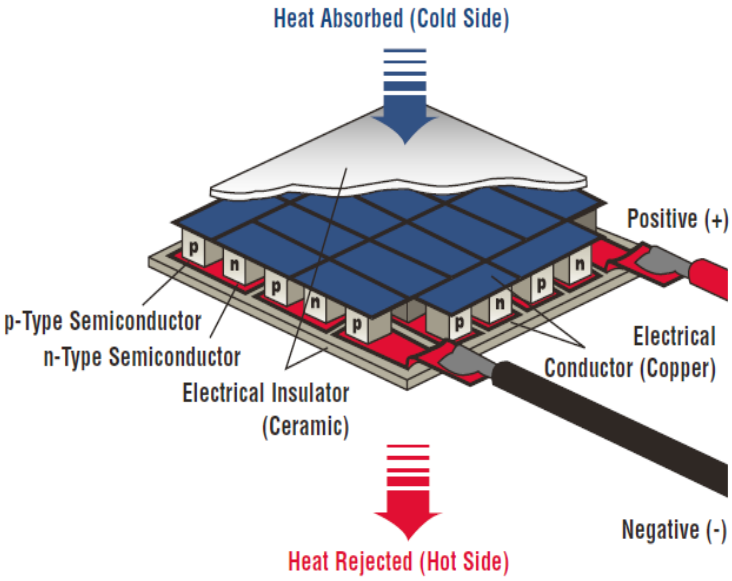

Figure 4.3 Internal structure of a thermoelectric cooler [35]

As the electrons move from the P type material to the N type material through an electrical connector, the electrons jump to a higher energy state absorbing thermal energy (cold side). Continuing through the lattice of material, the electrons flow from the N type material to the P type material through an electrical connector, dropping to a lower energy state and releasing energy as heat to the heat sink (hot side).

Thermoelectric can be used to heat and to cool, depending on the direction of the current. In an application requiring both heating and cooling, the design should focus on the cooling mode. Using a thermoelectric in the heating mode is very efficient because all the internal heating (Joulian heat) and the load from the cold side is pumped to the hot side. This reduces the power needed to achieve the desired heating [36].

4.3.1 Thermal Parameters

The heat pumping capacity of a TEC is given by,

$$Q_c = 2N\left(\alpha i T_c - \frac{i^2\rho}{2G} - K\Delta T G\right) \tag{4.7}$$

The amount of electric power which is dissipated as heat by a TEC in order to pump heat from the cold side to the hot side is given by,

$$Q_{TEC} = 2N\left(\frac{i^2\rho}{G} + \alpha i \Delta T\right) \tag{4.8}$$

In order to choose the right thermo electric module for an application. There are three parameters that need to be considered. They are the hot surface temperature (T_h), the cold surface temperature (T_c), and the heat load to be absorbed at the cold surface (Q_c).

The hot side of the TEC is the heat rejection side when a DC power is applied. This part is usually attached to a heatsink. Very often the heat sink is an important component in the assembly. A heat sink that is too small means that the desired cold side temperature may not be obtained.

The hot side temperature can be used by using the equations,

$$T_h = T_{amb} + (\emptyset)(Q_h) \tag{4.9}$$

$$Q_h = Q_c + Q_{TEC} \tag{4.10}$$

The cold side of the thermoelectric is the side that gets cold when DC power is applied. This side may need to be colder than the desired temperature of the cooled object. This is especially true when the cold side is not in direct contact with the object, such as when cooling an enclosure.

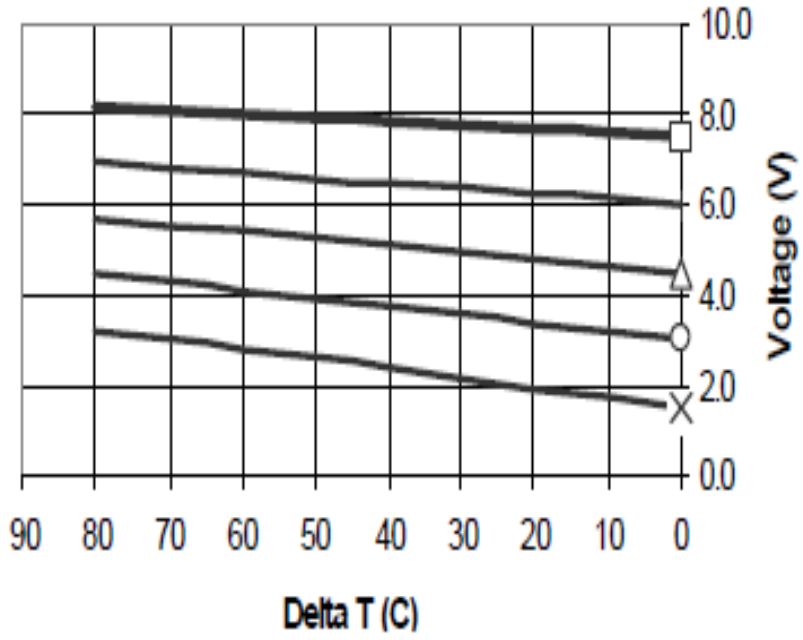

Figure 4.4 Performance curve for TEC showing voltage vs ΔT

The temperature difference across the thermoelectric is given by,

$$\Delta T = T_h - T_c \tag{4.11}$$

Thermoelectric performance curves are plotted with ΔT against voltage (V) and heat pumped (Q_c). Typical TEC performance curves are shown in Figure 4.4 and Figure 4.5.

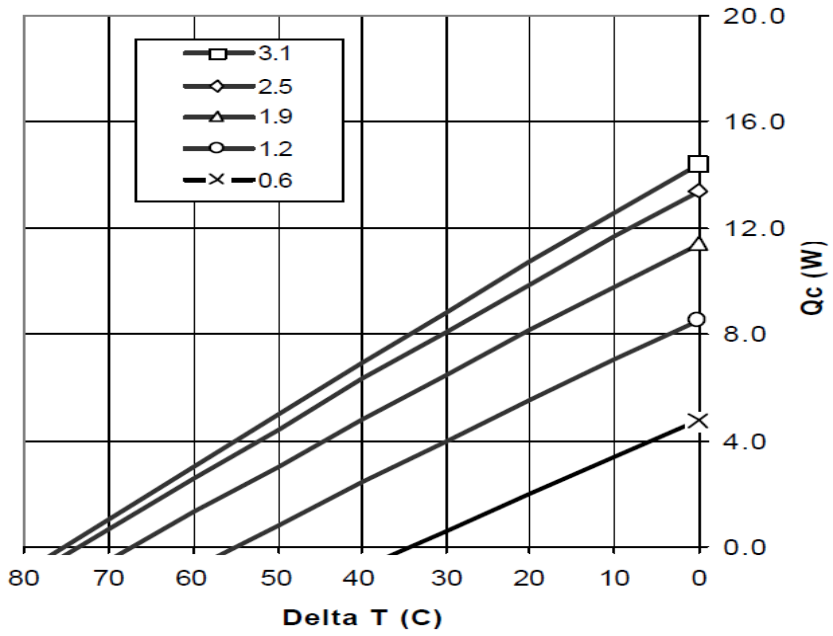

Figure 4.5 Performance curve for TEC showing heat pumped vs ΔT

4.3.2 Numerical Modeling of TEC

In Flotherm the TEC smart part is modeled as two cuboids which sandwich a layer of insulator in between as shown in Figure 4.6 [26]. Each of the cuboids corresponds to the hot side and cold side of the TEC. The insulation layer is to ensure that the heat pumped does not flow back to the cold side.

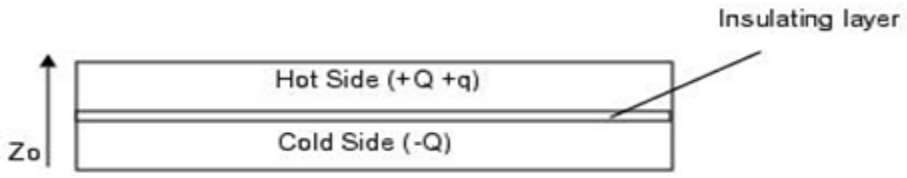

Figure 4.6 Schematic for numerical modeling of TEC

There are two kinds of input data for the smart part : the characteristic data which includes the maximum values of heat pumped (Qmax), delta T (ΔTmax), current (Imax) and voltage (Vmax), the second type of input date is the operational current.

CHAPTER 5

THERMAL DESIGN OF TELECOMMUNICATION CABINETS

5.1 Background

Commscope integrated cabinets provide environmentally secure enclosures for all types of electronic equipment. The cabinets optimize equipment density, heat transfer and dissipation, power reserve, environmental protection and ease of installation [37]. This study uses CFD analysis capabilities to provide design suggestions during the product development phase.

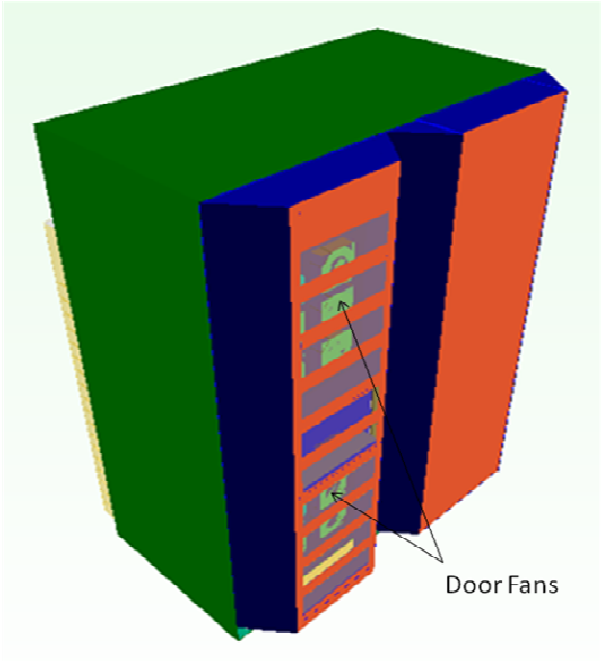

Figure 5.1 External view of a telecommunication cabinet

RBA84-3036 is a large-sized enclosure of CommScope's 'Integrated Cabinets Solutions' (ICS) product line. It is used to support wireline application in the telecommunication access network. The enclosure, which is approximately 66 inches wide, 84 inches high and 48 inches deep is divided into two compartments- a radio compartment on the left side and a battery compartment on the right side. The fully enclosed model is shown in Figure 5.1. The radio compartment houses some high power electronic components which are named, Radio Equipment 1 (RE1) and Radio Equipment (RE2) and also other passive components like the Power Distribution Unit (PDU) and radio filters.

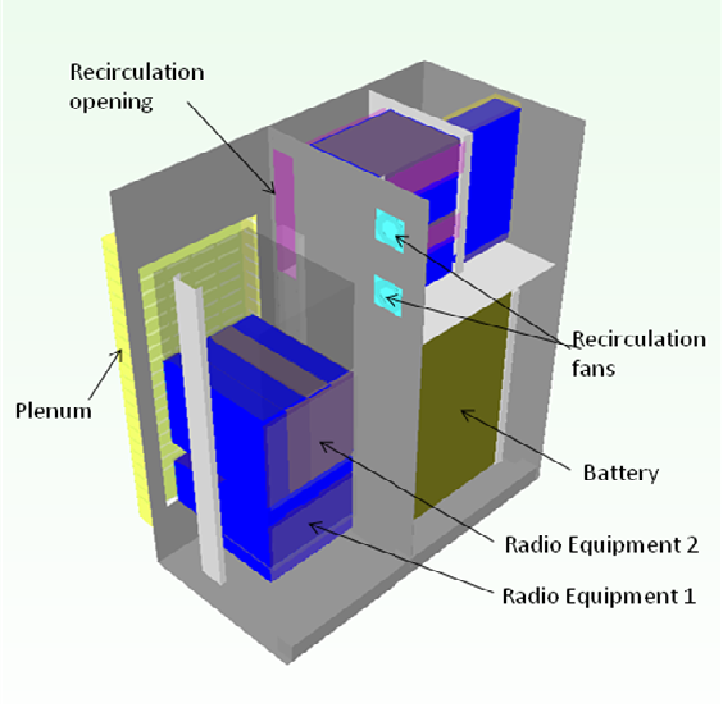

Figure 5.2 Internal components of the cabinet

Figure 5.2 shows internal components of the cabinet. The heat output of these components necessitates a robust forced convection cooling system. The door assembly in the radio compartment houses two fan tray assemblies, each comprising six DC axial flow fans. Each fan is capable of delivering a maximum air flow of 350 CFM and a static pressure of 0.96

in. of water. They deliver all the air flow required for cooling this cabinet. The filters are installed in the door assembly to keep out all the undesired particles and moisture from entering the enclosure. The battery compartment houses twelve strings of batteries with each string comprising of two 24V 180 Ahr batteries. The chamber above the batteries holds a DC power shelf, AC panel and a customer electronic unit that is capable of dissipating upto 400W of heat. The required air to cool these components is diverted from the stream of air that is delivered by the door fans by using either a system of baffle and opening or a set of two recirculation fans in the partition wall. The partition wall has a rear opening on the top side adjacent to the power shelf and the customer unit. The air after cooling the electronic components in the battery compartment is exhausted through the rear opening of the partition wall.

The high powered radio electronic equipments in the radio compartment have their own set of internal fans, which pull adequate amount of air to cool their internal components. This helps to prevent the bypassing of air delivered by the door fans which would otherwise choose the path of least resistance. There are five units of RE1 with two fans each at an operating point of 46 CFM, and four units of RE2 with five fans each at an operating point of 29 CFM.

All the air generated by the door mounted fans exit the enclosure through the rear air plenum. The plenum is provided with a system of actuated louvers, which prevents the entry of unwanted elements into the cabinet and also avoids the build-up of back pressure in the cabinet.

Solar loading has been applied based on the Telcordia GR-487 CORE standards, which states that 70 W/ft^2 should be incident on any three walls of the cabinet. Heater strips are used to simulate the effect of solar loading as done in an experimental setup. The heater strips are located on the top, right and the rear sides of the cabinet. In order to reduce the effect of heat buildup due to solar loading, insulation is provided on the inside of all walls, except on the front side of the cabinet.

5.2 Numerical Modeling

Detailed modeling of telecommunication cabinet of this size and complexity would result in millions of elements and a prohibitively long CPU time to solve the CFD model. Simplifying the complicated geometry without losing its characteristic behavior is necessary to minimize the solution time. In order to reliably reduce mesh counts and solution time, system level compact models of components need to be developed. Figure 5.3 shows the schematics of the modeling methodology [38].

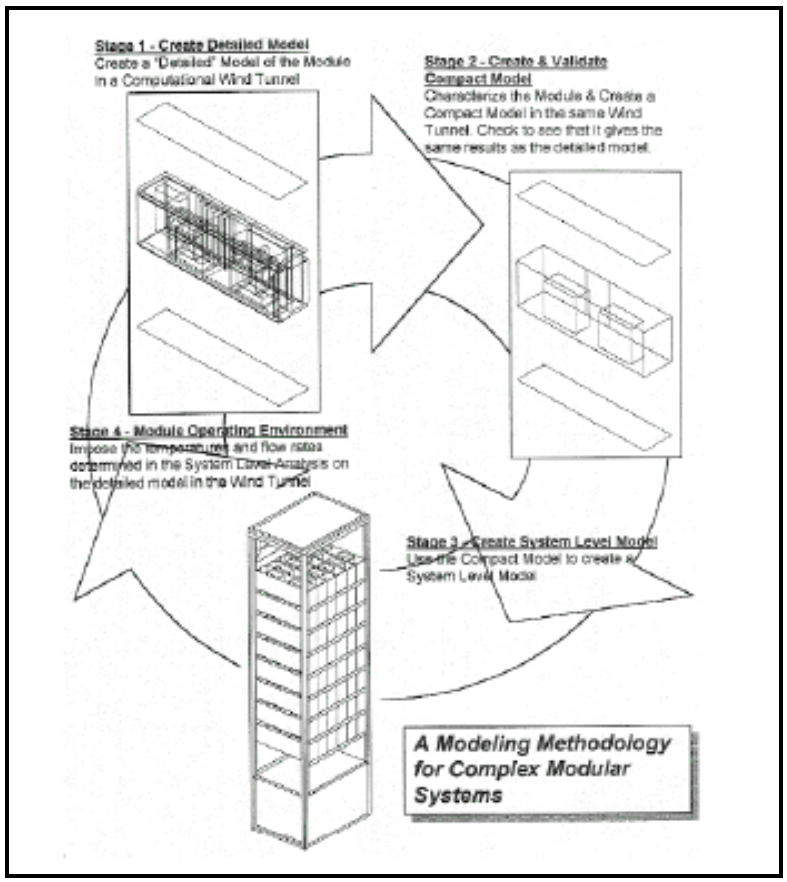

Figure 5.3 Schematic showing the compact modeling methodology

The cabinet is modeled as a large enclosure with a partition to separate the electronic and battery compartments. The solution domain is modeled with twice the height of the cabinet and an additional one-half the width and depth of the cabinet on all the four sides. All the five sides of the domain are modeled with open walls except the bottom surface which is given a no slip condition. The ambient temperature is set to 50ºC to simulate the worst case scenario. For the air-flow automatic algebraic or the LVEL turbulence model is used. The effect of radiation is turned off as the primary mode of heat transfer is assumed to be convection and conduction.

All the electronics equipment has been modeled as compact models with cubical enclosures having openings on the front and rear end. The system impedance of these components is modeled with advanced resistance macros in Flotherm, which incorporates the pressure drop characteristics of the equipment. The system impedance curve is obtained from experimental wind tunnel testing, and is further illustrated in Appendix A. While monitoring the thermal data, it is to be noted that only the temperatures surrounding the compact models are accurate. The temperature inside the compact models is not considered for the analysis [39].

The fans are modeled by using the fan smart part and are given the fan performance curve so that the correct operating point is attained in the analysis. The filter consists of two layers the first is a particulate filter and the second one is a hydrophobic filter. They are modeled with volumetric resistances as explained in chapter 4.

5.3 Numerical Analysis

CFD modeling has been used to perform a range of thermal/airflow analysis as shown in Figure 5.4 the first part of the analysis is a feasibility study which compares two different cooling systems for the battery compartment. The second part is a series of parametric studies where different sizes, numbers and flow rates of axial door fans, rear plenum, recirculation opening and circulation fan has been studied.

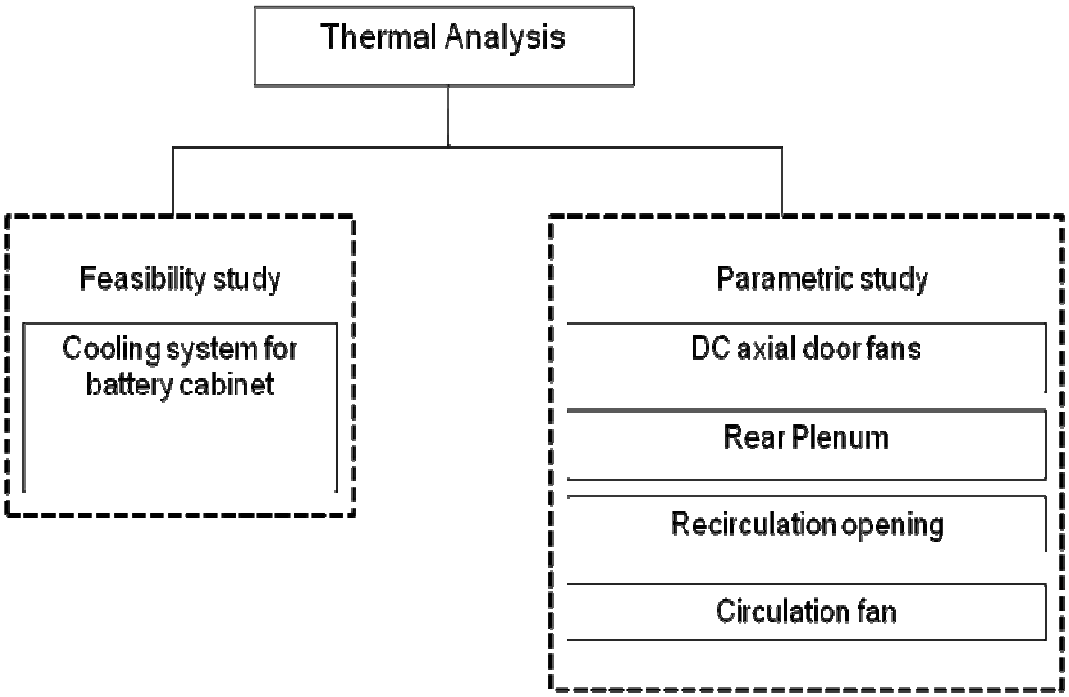

Figure 5.4 Schematic showing the thermal analysis

5.3.1 Comparison of Two Cooling Systems for the Battery Compartment

The battery compartment of the cabinet is to be cooled with air delivered by the door fans in the radio compartment of the cabinet. An initial study was done to find the feasibility of using a baffle/opening system (shown in Figure 5.5) to divert a part of the ambient air supplied by the axial door fans. CFD analyses for two cases were compared, the first case uses the baffle/opening system and the second case uses recirculation fans on the partition wall.

The data indicates that the baffle did not deflect enough air into the battery compartment. The main reason for this was much of the air from the fans was directed onto the radio electronics and the remaining air-flow bypassed both the electronics and the inclined baffle. Measurements which were taken with the aid of the volume region on the recirculation opening showed that the air-flow was quite contrary to expected behavior. The air was actually going into the battery compartment through the rear opening of the partition wall and

recirculating back through the front opening. This led to extremely high inlet and exit temperatures in the power shelf and the customer electronic unit.

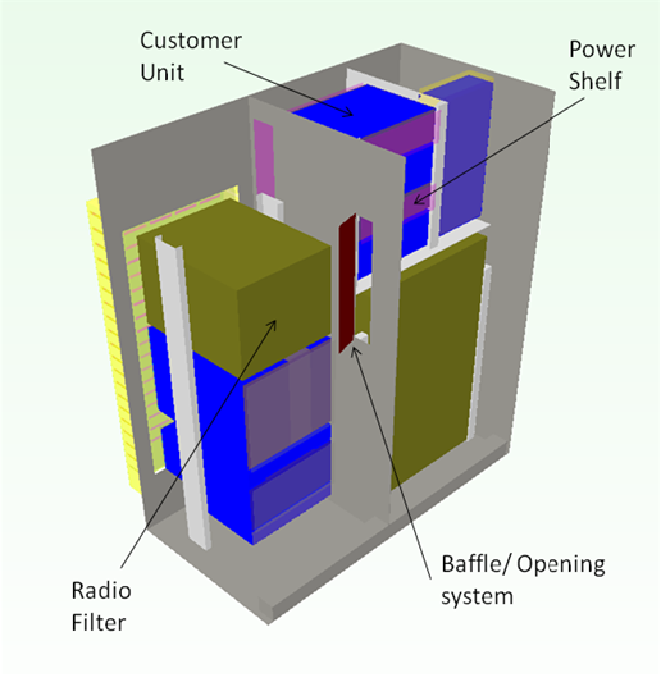

Figure 5.5 Cabinet with the baffle/opening system

The recirculation fans were located closer to the power dissipating units of the battery compartment. These fans were mounted on the partition wall. This construction proved to be adequate to limit the air inlet temperature to the battery compartment to 60ºC and to meet thermal budget target of 15ºC for the power shelf and customer unit. Hence, recirculation fans were chosen as a suitable cooling system for the battery compartment electronics. The results for this feasibility study are shown in Table 1. Parametric study was performed for the flow rates of the partition wall fans and is discussed later.

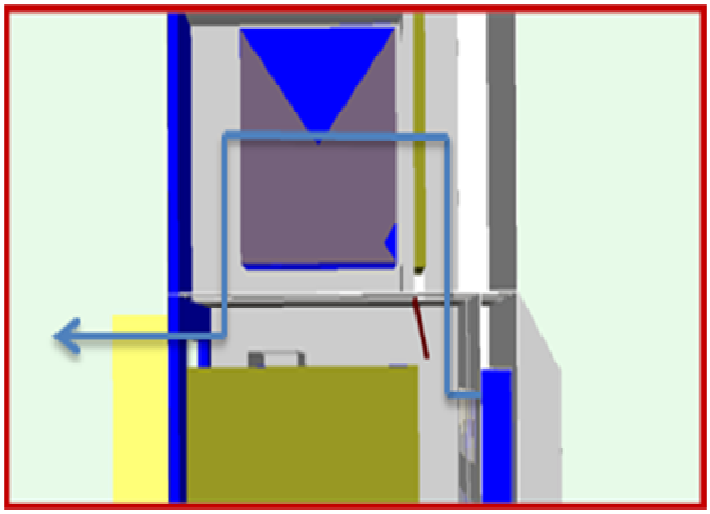

Figure 5.6 Expected air-flow using the baffle/opening system

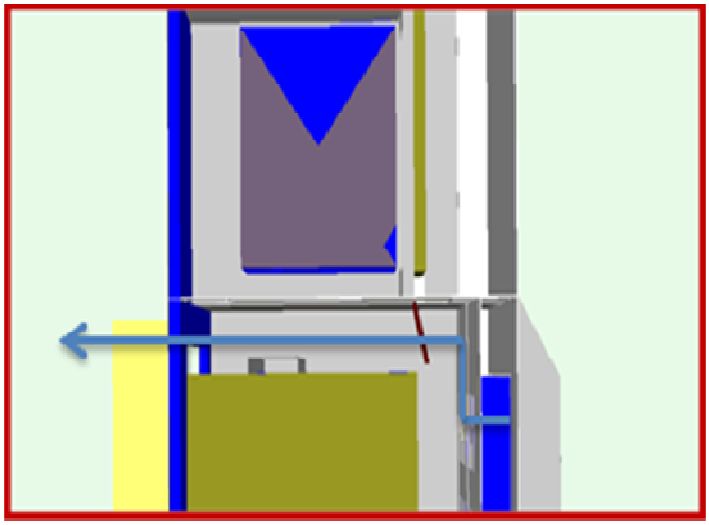

Figure 5.7 Actual air-flow using the baffle/opening system

Figure 5.6 and Figure 5.7 shows the expected air-flow path and the actual air-flow path from the radio compartment. It was observed all the electronics in the radio compartment showed temperature below 60ºC and it was only the electronic components in the battery

compartment that showed higher temperatures. Hence only the temperatures for the latter are reported here.

Table 5.1 Comparison of Cooling System for the Battery Compartment

Cooling system	Power Shelf inlet (^{0}C)	Power Shelf outlet (^{0}C)	Cust. unit inlet (^{0}C)	Cust. unit outlet (^{0}C)
Baffle/opening	71.7	88.8	142.7	105.5
Recirc. Fan	55.2	76.8	55.4	65.8

Figure 5.8 and Figure 5.9 show the vector plots for the baffle/opening system and recirculation fan system respectively.

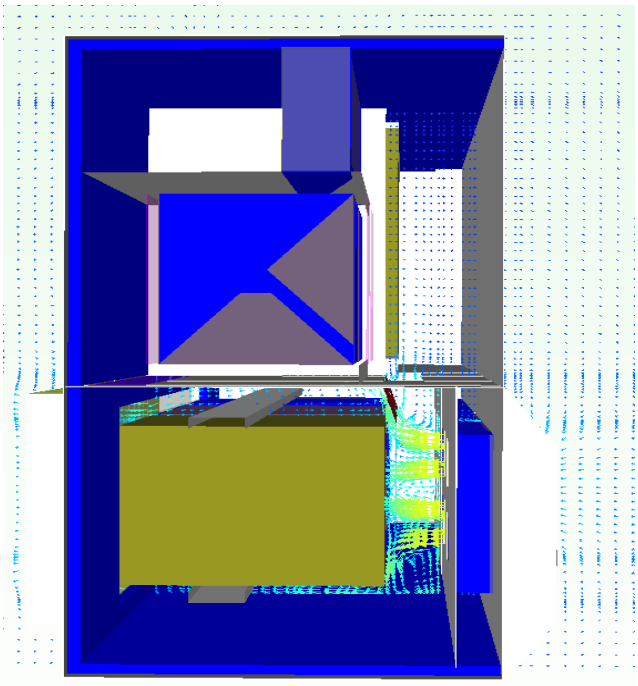

Figure 5.8 Vector plot showing the air-flow using the baffle/opening system

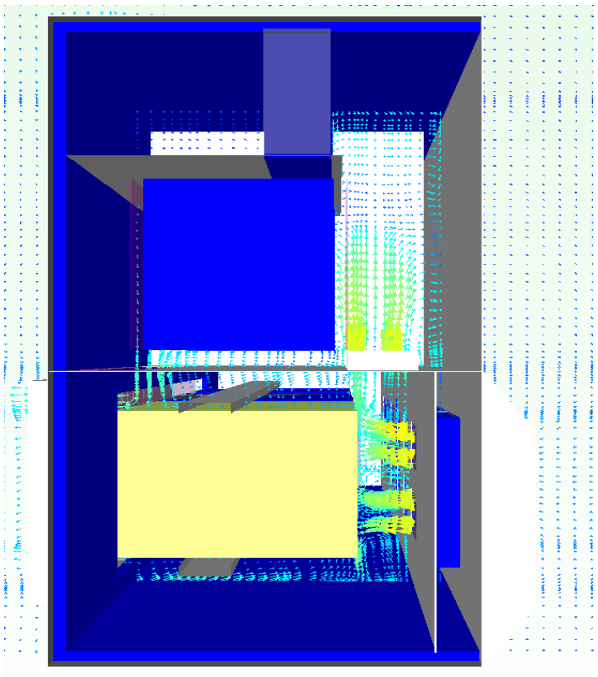

Figure 5.9 Vector plot showing the air-flow using the recirculation fan system

5.3.2 Axial Door Fan Arrangements

A study was performed to find the effectiveness of cabinet cooling with different number and positions of door fans. The room to move the fans horizontally was restricted by the condition that the fans have to be positioned directly in front of the cabinet electronics. Hence the positions were varied in the vertical direction only. Also, a symmetrical arrangement of the fans on the upper and lower half of the cabinet door was considered, taking into account the manufacturing cost savings for such a configuration. Four different door fan configurations were considered with two 8 fan configurations, one 10 fan configuration and one 12 fan configuration.

For the first 8 fan configuration, the vertical and horizontal spacing was kept at 3.88 inches and 3.16 inches respectively. This configuration is denoted by 8 fans (1) in Table 2. For the second 8 fan configuration the vertical and horizontal spacing was 7.88 inches and 3.16 inches respectively. This configuration is denoted by 8 fans (2) in Table 5.2. All the fan configurations are shown in Figure 5.10 and Figure 5.11.

For all the four configurations the inlet and exit temperatures of the electronics in the radio compartment showed fairly similar values, with the 10 fan configuration providing the best results.

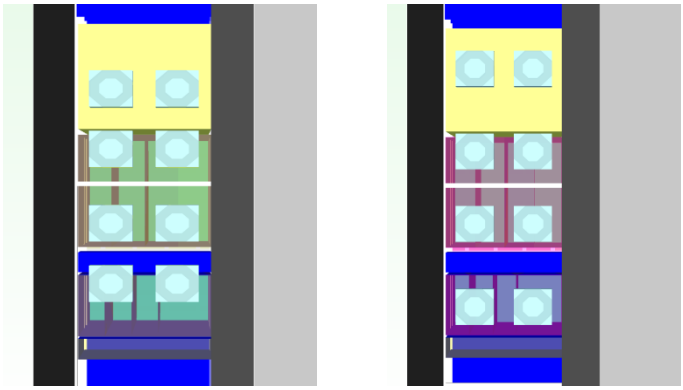

Figure 5.10 8 fans configuration- 8 fans(1) and 8 fans(2).

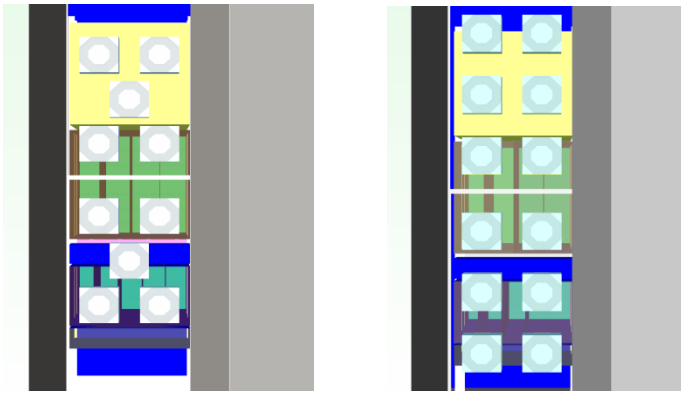

Figure 5.11 10 fan and 12 fan configuration.

However, it needs to be seen how the 10 fan configuration would provide the redundancy in the case of a possible fan failure, given the orientation of fans in that design. Considering the redundancy factor, the 12 fan configuration was chosen for the cabinet design. Also in the event of greater heat accumulation due to a higher population of electronics in the cabinet, the 12 fan configuration is more likely to provide adequate thermal management.

Table 5.2 Results for Axial Door Fan Arrangement

No: of fans	Power Shelf inlet (^{0}C)	Power Shelf outlet (^{0}C)	Cust. unit inlet (^{0}C)	Cust. unit outlet (^{0}C)
8 fans (1)	55.4	76.1	54.1	64.5
8 fans (2)	55.1	77.3	53.8	62.4
10 fans	54.9	75.8	53.4	64.5
12 fans	55.2	76.8	55.4	65.8

5.3.3 Parametric Study of Rear Opening and Plenum height

The hot exhaust air of the cabinet exits through the rear opening on the radio compartment and passes through the plenum area which has a patterned set of actuated louvers. A parametric study to find the effect of varying the height of the rear opening and plenum on the inlet and exit temperatures of the cabinet electronics was performed. While varying the height, a gap of 3 inches between the top edges of the rear opening and plenum was always maintained i.e. if the height of the rear opening was 55 inches the plenum height would be 58 inches. The width of the opening was always maintained at 23.5 inches.

The height of the rear opening was varied from 37 inches to 58 inches. As the exit and inlet temperatures of the radio side electronics showed no appreciable changes for different heights, the temperature values for the power shelf and the customer unit were the main criteria for selecting the right dimensions.

As can be seen from Table 5.3, with increase in opening height both the inlet and exit temperatures of the electronics in the battery compartment showed a decrease. This is attributed to the better scavenging of the exhaust air from the battery compartment. The plenum height could not be increased all the way to the top as space had to be provided above the plenum on the rear side of the cabinet for a small box that housed the RF cables and the

connectors which communicates the RF signals to and from the antenna. Therefore the optimum height of 55 inches was chosen for the rear cabinet opening.

Table 5.3 Results for the Parametric Study of Rear Opening and Plenum Height

Height (inches)	Power Shelf inlet (^{o}C)	Power Shelf outlet (^{o}C)	Cust. unit inlet (^{o}C)	Cust. unit outlet (^{o}C)
58	54.4	76.5	54.1	63.7
55	55.2	76.8	55.4	65.8
52	55.8	77.5	57.2	67.6
49	56.2	78.1	57.7	68.2
46	56.2	80.7	58.1	68.7
43	56.5	81.1	58.2	68.9
40	56.2	80.8	57.4	68.1
37	57.2	81.3	59.2	69.9

5.3.4 Parametric Study of the Recirculation Opening

The recirculation opening is located on the rear top side of the partition wall. It serves to exhaust the hot air generated from the power shelf and customer electronic unit in the battery compartment. The hot air exhausted from the battery compartment had to take a tortuous path, as it has to turn 90^{o} to exit through the recirculation opening, moving out through a narrow channel between the filter radio and the partition wall before it exhausts through the rear plenum. Therefore, optimizing the size of the recirculation opening is important in order to avoid the buildup of heat in the battery compartment.

Table 5.4 Results for the Parametric Study of Recirculation Opening

Height (inches)	Power Shelf inlet (^{o}C)	Power Shelf outlet (^{o}C)	Cust. unit inlet (^{o}C)	Cust. unit outlet (^{o}C)
25	55.2	76.8	55.4	65.8
22	55.1	76.2	55.8	65.5
19	55.1	76.3	55.9	64.4
16	55.4	77.5	56.4	63.9
13	56.8	80.3	57.1	63.4
10	58.7	82.7	57.1	63.2

For the parametric study, the initial size of the recirculation opening was kept at the maximum possible size. Given the physical constraint, this size was kept at 25 inches. In subsequent steps, the size was decreased by 3 inches to a minimum of 10 inches. In all the cases the width of the opening was kept at 4.5 inches. The parameters that were considered were the exit temperatures of the power shelf and customer unit. The rest of the monitored temperatures seemed to be unaffected by the change in the recirculation opening size. Results are shown in Table 5.4. The most suited result was for the 19 inch opening when both inlet and exit temperatures were considered.

5.3.5 Parametric Study of the Recirculation Fan

The air to cool the battery compartment is supplied by the recirculation fans placed on the partition walls. These fans are located near the power dissipating units of the battery compartment. The air from these fans is supplied parallel to the face of these units. There is much less flow bypass due to the restricted space in the top of the battery compartment. The static pressure build up due to the restricted space ensures that air is delivered into the power

units. This parametric study aims to find the required amount of flow rate so as to maintain the electronics within the stipulated thermal budget.

Table 5.5 Results for the Parametric Study of Recirculation Fan

Flow rate (CFM)	Power Shelf inlet (^{o}C)	Power Shelf outlet (^{o}C)	Cust. unit inlet (^{o}C)	Cust. unit outlet (^{o}C)
50	66.5	105.4	105.1	122.7
100	56.7	81.4	59.2	81.5
130	55.8	77.7	56.5	68.2
140	55.5	76.8	56.4	66.1

The results shown in Table 5.5 indicate that a flow rate close to 140 CFM is required. Hence choosing a fan which would provide an operating point of this value is needed to maintain the electronics in the prescribed temperature regime.

5.4 Conclusion

Modern standalone environmental cabinets house high density of electronic components which dissipate a large amount of heat. Careful design of the cabinet is called for to ensure that the electronics function within the prescribed operating range, and does not cause early product failure. CFD analysis aids to make quicker design decisions without expensive prototype testing. Compact models are used in place of detailed geometry for system level modeling. This simplifies the model thereby saving on computational cost and time.

In this paper, a feasibility study was performed to evaluate two types of cooling systems for the battery compartment of the cabinet. The baffle/opening system proved to be inadequate in cooling the battery compartment electronics; whereas the recirculation fans ensured that the temperatures were kept within desired limits. Also various parametric studies were performed to determine the optimal number and position of the axial door fans, height of rear opening and plenum, height of recirculation opening and required flow rate of recirculation fans.

CHAPTER 6

MODELING METHODOLOGY FOR THERMOELECTRIC COOLER AIR-AIR ASSEMBLY

6.1 Background

A typical telecommunication cabinet provides a secure enclosure for various types of electronic components and back-up batteries. The cabinet should provide an environment in which these components could function reliably. In addition to providing the right amount of air within the prescribed temperature, thermal management of the cabinet should ensure that the battery compartment should be maintained at close to its optimum working temperature (25^{o}C). Many a times, this requires cooling the battery compartment below ambient temperatures. Two of the most common ways to do this is to use either vapor compression refrigeration or use TEC refrigeration. TECs provide the advantage of being highly reliable and quite in operation, two qualities that are important for stand-alone telecommunication cabinets. The TEC devices are employed in conjunction with heat sinks and fan. It is an indirect method of cooling and therefore takes a long time to bring down the battery temperature[40]. This study discusses the thermal management of the battery compartment of an outdoor telecommunication cabinet using air-air TEC heat exchangers. A novel method to model these air-air TEC exchangers using a commercial CFD code is also discussed.

Telecommunication cabinets with their multiple equipment configurations require numerous tests and analysis to ensure an acceptable thermal performance. Prototype based experimental testing is usually time-consuming and can span several weeks. Using computational fluid dynamics, and with the advent of relatively low-cost and high powered computing capabilities, testing a large enclosure with multiple configurations can be accelerated through simulation. Though CFD might not give a pin-point accurate result, it does aid in giving

a qualitative assessment, thereby expediting the design process. The CFD code FLOTHERM by Mentor Graphics [42] is used for the thermal/airflow analysis in this study.

6.2 Model Description

6.2.1 Baseline Model

The telecommunication cabinet in this study has dimensions measuring approximately 30 inches wide, 48 inches high and 35 inches deep (shown in Figure 6.1). It is manufactured by Commscope Solutions Inc. [37]

The equipment inside the cabinet is a function of application to be served. The cabinet discussed in this study consists of the electronic equipment, rectifier shelf, Heat Exchanger (HX) and inner/outer loop fan trays and Thermo Electric Cooler (TEC) modules. The electronic equipment and the rectifier shelf consist of numerous circuit cards, whose active components dissipate heat. The customer shelf and rectifier dissipate the majority of heat in the cabinet.

Figure 6.1 External view of the telecommunication cabinet

The cabinet has two fan assemblies:

1. Bay fan tray (Inner loop, 3 fans)
2. HX fan tray (Outer loop, 2 fans)

The bay fan tray creates the inner loop air flow, i.e. pulls in internal air from the bottom of the electronic equipment and exhausts the hot air to the intake of the HX. So the air enters the inner loop of the HX from the top and after it has undergone cooling, is again rejected to shelf inlet from the HX exhaust. On the outer loop side, the HX fans pull ambient air from the bottom side of the HX and the flow is from bottom to top. While air is flowing through both the respective loops, heat transfer takes place following the counter-flow HX principle cooling the inner loop air. The warmer outer loop air is exhausted to the atmosphere. This cycle continues and the cooling medium (air in this case) never mixes. For both electronic equipment and rectifier shelf air inlet is through bottom and exhausted through the top. The electronic must be operated in tight thermal specifications in order to provide sufficient reliability and performance.

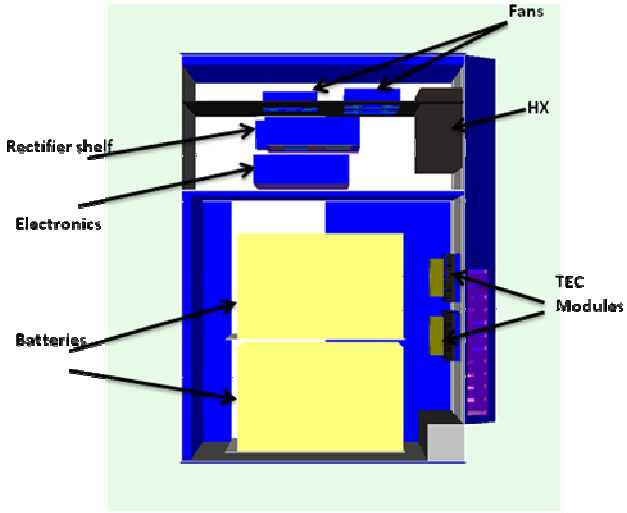

Figure 6.2 Internal components of cabinet (side view)

The bottom compartment of the cabinet houses the batteries. The cabinet is sealed from the external environment and is cooled by means of two TEC air-air exchanger units (see Figure 6.2). The details of the TEC exchanger units are explained in the next section. The battery compartment also houses electronic equipment, which is located in between the two sets of batteries. The power rating for this equipment is 50 W. Heater strips are used to simulate

the solar load. Heater strips are placed on three sides of the cabinet top, rear and right side. The solar load is applied only on three sides of the cabinet. The reason for this is, for any orientation of the cabinet, sun light will be incident only on the three sides at any given instant. Solar loading involves all the three forms of heat transfer and is given by sum of radiation, convection and conduction heat loads. The radiated heat load remains always positive and the direction of the convective and conductive heat loads depends on the cabinet temperature[42]. There has been considerable discussion going on in industries to account for solar load during testing. In this study the Telcordia[10] standards GR 487 CORE have been used to account for solar loading. According to this standard 70 W/ft^2 is applied to the three sides of the cabinet. In order to minimize the effect of the solar load, 1 inch insulation is provided on the inside walls of the cabinet.

6.2.1.1 Numerical Modeling

Thermoelectric coolers are modeled using the TEC smart part in Flotherm. It is constructed as a simple geometry with an insulating layer sandwiched between two cuboids. The cuboids represent the hot and cold side of the TEC. This is explained in detail in Chapter 4. The TEC air-air heat exchanger assembly used in this study consists of five main components 2 sets of fans, 2 heat sinks and the TEC cooling unit. This assembly is housed on the front wall of the battery cabinet with one set of heat sink and fan inside the cabinet, forming the inner loop and the other set of heat sink and fan on the outside; forming the outer loop .This arrangement is called the through-wall mount and is shown in Figure 6.3. Both the fans impinge air directly onto the heat sinks. The TEC cooling unit houses 8 TEC modules and they are electrically connected in a parallel-series network as shown in Figure 6.4.

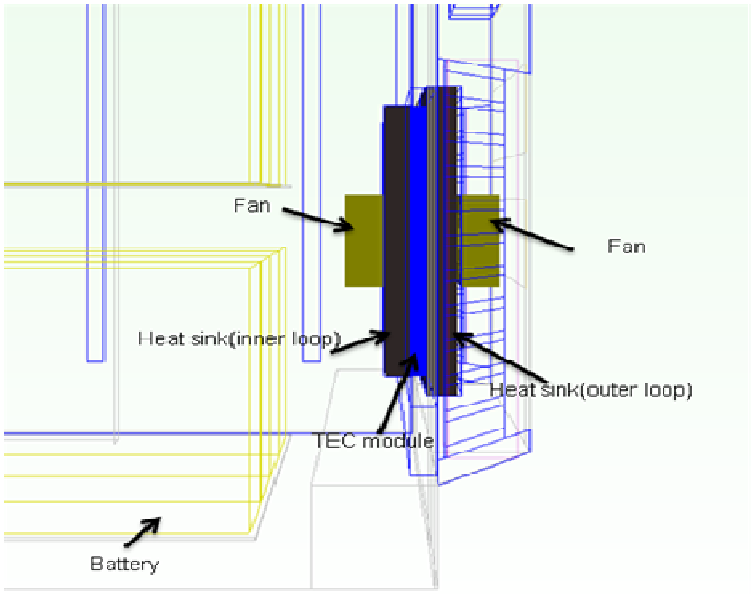

Figure 6.3 TEC air-air exchanger shown as a through-wall assembly in the cabinet (side view)

The TEC assembly is operated under a voltage of 54 V DC and the current drawn by the assembly at this voltage is approximately 8 A. With the nature of the parallel-series network each TEC module is subjected to a voltage drop of 13.5 V and draws in a current of 4 A. Here the assumption is that each TEC module has the same resistance (R_m) and there is no voltage drop across the wiring in the TEC cooling unit.

Table 6.1 Heat Loads of Electronic Components

Heat Load for electronic components (W)	
Rectifier Shelf	300
Electronics	250
Battery Electronics	50

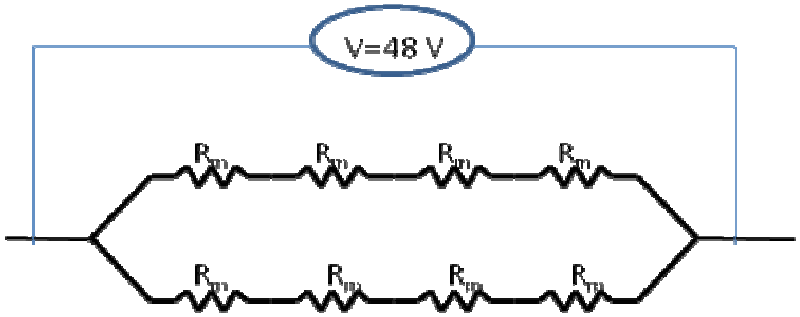

Figure 6.4 Electrical circuit diagram for the TEC modules inside the cooling unit

Often the characteristic data for the TEC modules is not provided by the manufacturer and it becomes difficult to model the TEC module as a smart part explicitly. A method to overcome this difficulty is to use one of the TEC smart part given in the Flotherm library. The Flotherm library has a list of commercially available TEC modules. Here the key is to select a TEC module which has a maximum voltage rating close to the maximum voltage rating of the module used in the actual assembly. This parameter is often available from datasheets provided by the manufacturer. The TEC module used for numerical modeling in this study is Melcor UT 8-12-30-F2 [35]. It should be noted that the maximum current rating for the numerical module should be higher than the operating current of the actual TEC module. It is widely observed that TECs have a better heat pumping efficiency when the operating current is 40-70% of the maximum rated current. The TEC smart part used for numerical analysis in this model has a maximum voltage rating of 14.4 V and a maximum current rating of 7.9 A.

The heat sinks that are used in the TEC air-to-air heat exchanger are modeled in detail with exact replication of the fin count, spacing and dimensions. Also the heat exchanger in the electronics compartment are modeled in detail. The batteries are modeled as cuboids which serve as to block the air-flow and produce no heat output. The electronics are modeled with enclosures with two faces open to facilitate the air-flow inside them. The pressure drop across them is modeled with resistances and the heat output is modeled with a heat source for their entire volume.

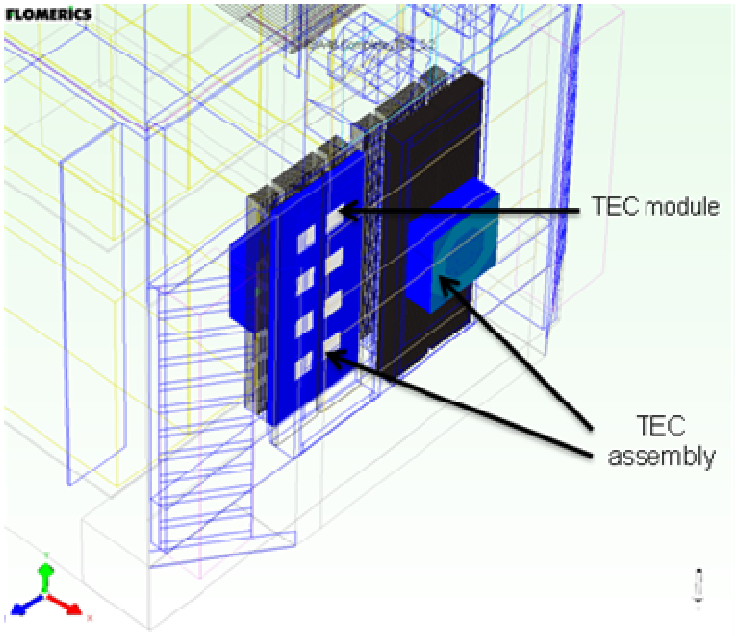

Figure 6.5 Internal view of the TEC air-air exchanger

Through this method of reverse engineering, the attempt is to replicate the characteristic behavior of the actual TEC module as close as possible. Figure 6.5 shows the two TEC assemblies with the assembly on the left showing the TEC cooling unit with the 8 individual TEC modules. It should be noted that the cooling unit is not represented by a detailed model instead it is modeled in such a way as to embody the functionality of the device.

6.2.2 Cabinet Model with Cowling and Baffles

In order to have a comparative study a model with a cowling for the fans of the TEC assembly and set of baffles in the battery cabinet was developed. This was hypothesized to give better results by cutting down on recirculation of air back into the fans in the TEC assembly. The cowling on the inner loop of the TEC forces the fans to draw hot air from between the two sets of batteries and prevents the cold air flowing out from the top of the heat sinks from being sucked back in. A similar cowling arrangement is provided on the outer loop of the TEC assembly. A set of two baffles are provided on the inside of the battery compartment,

between the side walls and the batteries, to supplement the cowling in reducing recirculation. This arrangement is shown in Figure 6.6 and Figure 6.7.

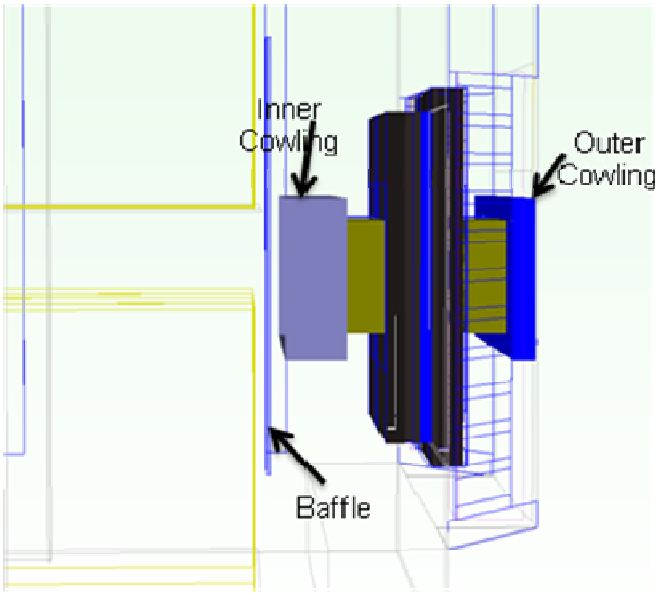

Figure 6.6 TEC assembly with the cowlings (side view)

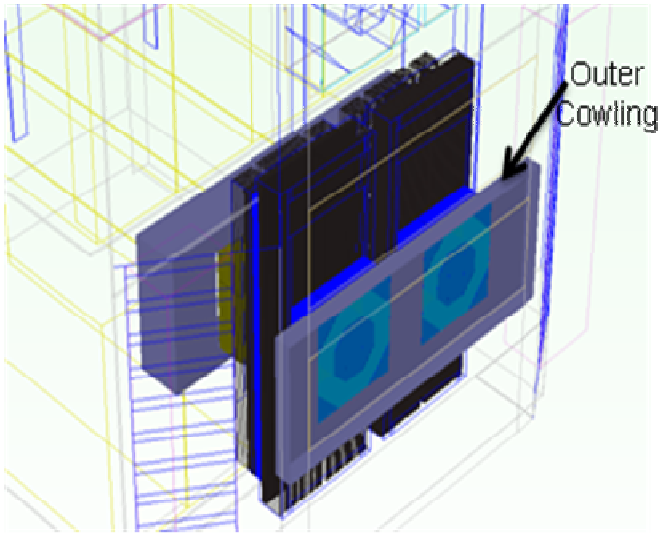

Figure 6.7 TEC assembly with the cowlings (isometric view)

6.3 Results

The focus of this study is on the cooling of the battery cabinet. In the experimental analysis, the temperature readings in the cabinet were taken using thermocouples. The most critical temperature is the battery temperature, and the readings were taken for the guideposts of the batteries. This location was expected to give the closest value to the actual battery temperature. In the numerical analysis the functionality of the thermocouples were mimicked using monitor points. They were located close to the top and 10 mm in front of the batteries. The approximate location of the monitor points are shown in Figure 6.8. The upper monitor points are numbered 1-1, 1-2, 1-3 and 1-4, while the lower monitor points are numbered 2-1, 2-2, 2-3 and 2-4.

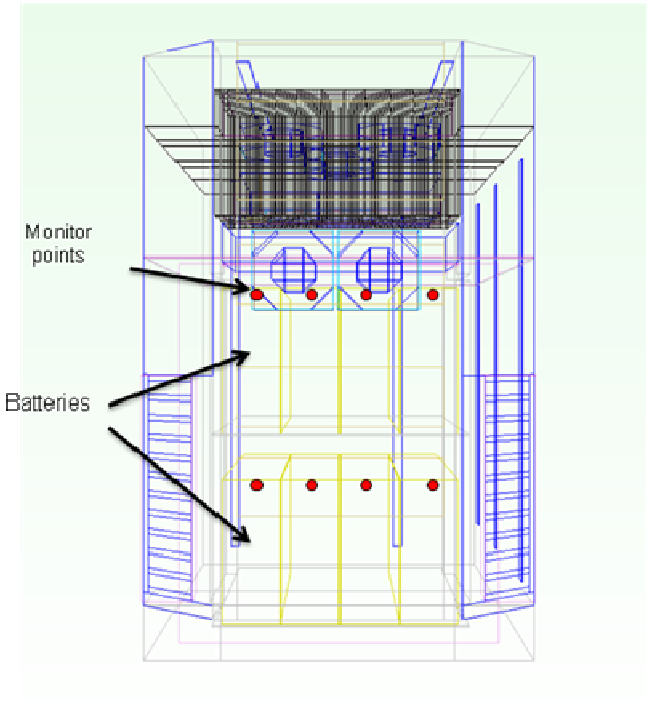

Figure 6.8 Front view showing monitor point locations

Replicating the actual test environment in the test chamber, the ambient temperature for the numerical model was set to 38 ºC and modeled with still air. The test results with the baseline case and the model with TEC assembly cowling and baffles were obtained and compared with similar experimental test results. The experimental data was provided by the cabinet manufacturer.

For ease of tabulation the base model, with no ducting in the form of cowlings and baffles, is reported as Case 1 and the model with the ducting accessories is referred to as Case 2.

Table 6.2 Comparison of Numerical and Experimental Results for Case 1

	Case 1	
	Numerical (ºC)	**Experimental (ºC)**
Battery 1-1	40.2	40.2
Battery 1-2	39.8	40.2
Battery 1-3	38.0	39.1
Battery 1-4	39.0	39.4
Battery 2-1	37.9	39.8
Battery 2-2	37.4	39
Battery 2-3	37.0	38.8
Battery 2-4	37.9	39.2

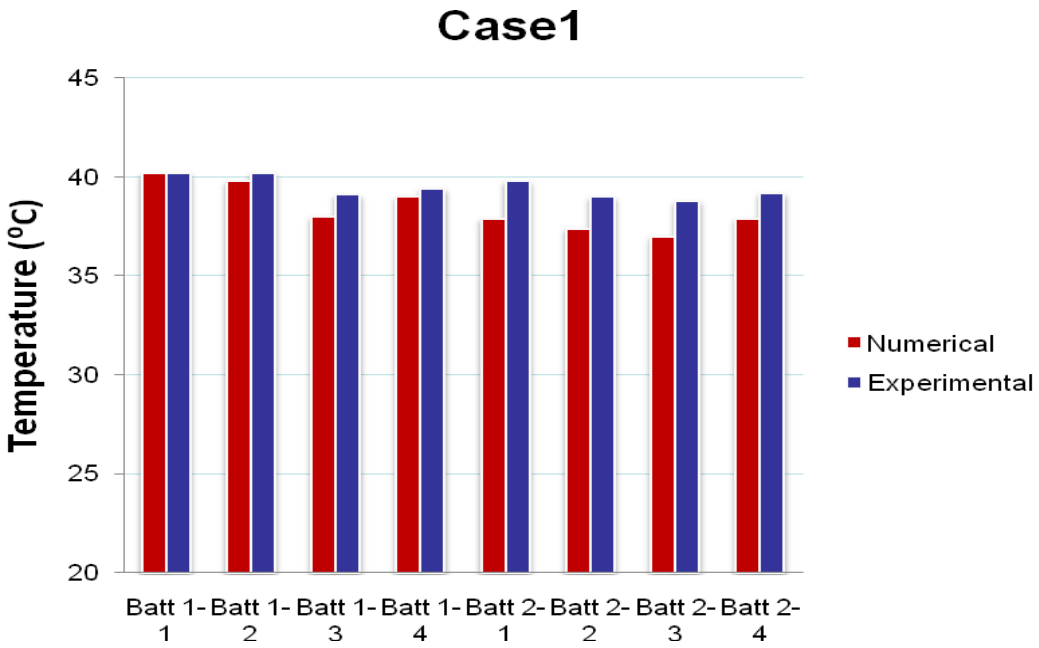

Figure 6.9 Comparison of numerical and experimental results for case 1

Table 6.3 Comparison of Numerical and Experimental Results for Case 2

	Case 2	
	Numerical (°C)	**Experimental (°C)**
Battery 1-1	37.4	36.1
Battery 1-2	37.0	35.7
Battery 1-3	35.1	35.2
Battery 1-4	36.0	35.6
Battery 2-1	34.3	35.2
Battery 2-2	33.3	35
Battery 2-3	34.2	35.6
Battery 2-4	35.5	36.5

Figure 6.10 Comparison of numerical and experimental results for case 2

Table 6.2 and Table 6.3 shows the comparison of numerical and experimental data for the two cases mentioned earlier. In both the cases the numerical data shows a good degree of closeness with the experimental data. The values show a difference of less than 5 percent. Part of this difference could be attributed to the air leakages in the experimental model. An observation that is to be made here is that on comparing the experimental results between Case 1 and Case 2, there is a difference of approximately 3.5ºC between the temperature values. A similar trend is also shown by the numerical results. The closeness in values and similar trends for both the cases, between numerical and experimental results, shows that there is a fair degree of consistency with the numerical data.

Figure 6.11 and Figure 6.12 shows the vector plots for case 1 and case 2. It is clearly seen in Figure 6.12 that the cowlings around the TEC assembly do a good job in cutting down on recirculation. This reduction in recirculation leads to an approximately 3ºC drop in temperatures in the battery compartment.

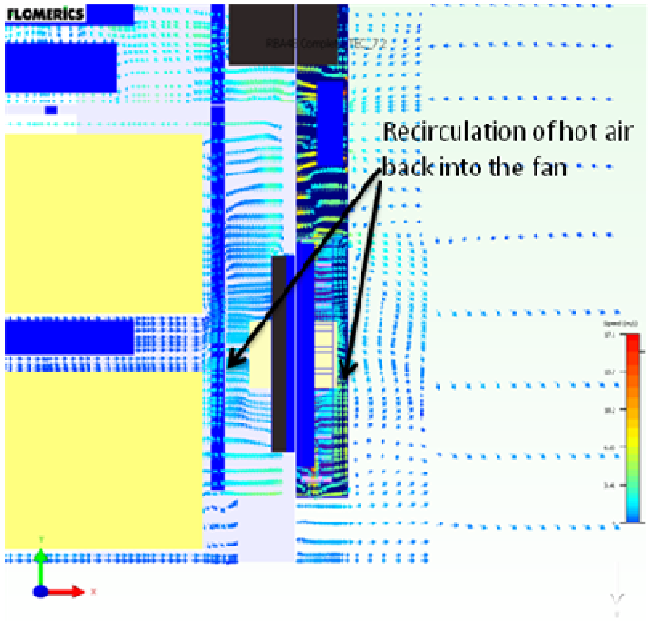

Figure 6.11 Vector plots for case 1(side view)

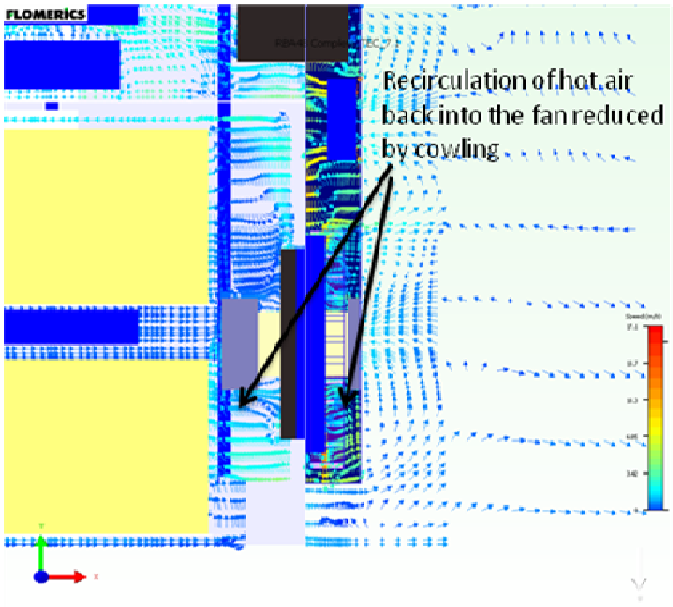

Figure 6.12 Vector plots for case 2(side view)

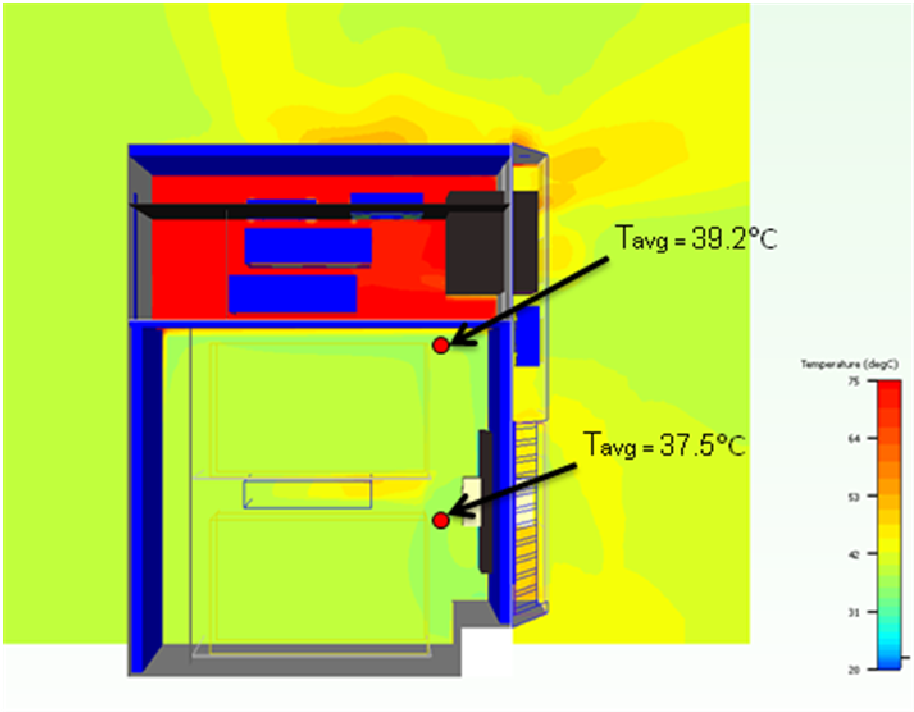

Figure 6.13 Thermal plots for case 1(side view)

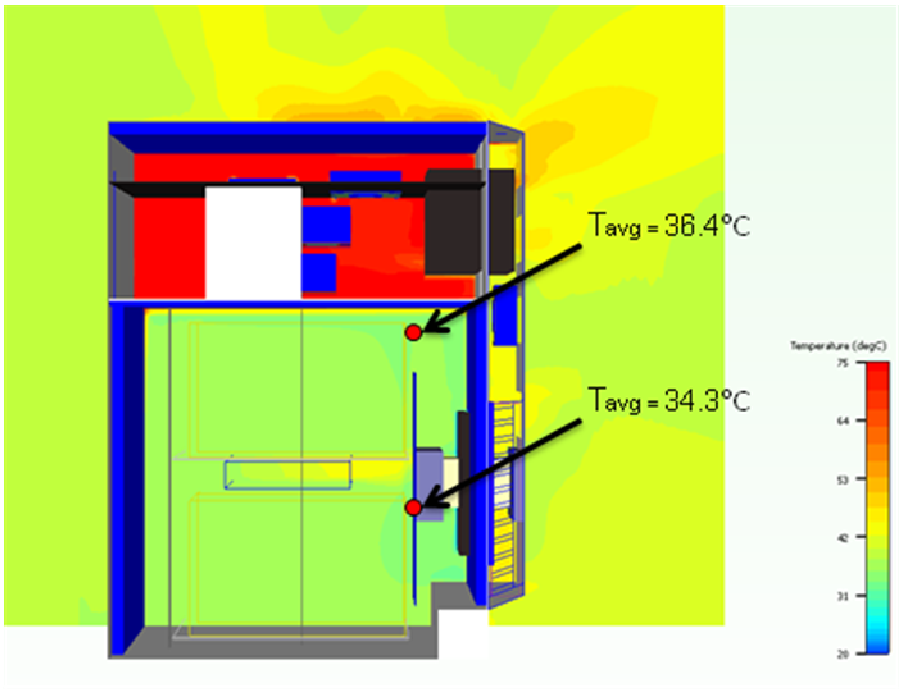

Figure 6.14 Thermal plots for case 2(side view)

In order to understand the impact of failure of one or both of the TEC assemblies, three different scenarios were considered. The first scenario has the TEC assembly on the left side of the battery compartment as the failed unit and the battery temperatures are reported as Case 3. The second scenario has the right TEC assembly failed and the third one has both the TEC assemblies failed, these scenarios are reported as Case 4 and Case 5 respectively. The various monitor point readings are shown in Table 6.4.

Table 6.4 Comparison of Numerical Results for Various Cases of TEC Assembly Failures

	Case 3 (ºC)	**Case 4 (ºC)**	**Case 5 (ºC)**
Battery 1-1	46.5	51.3	73.1
Battery 1-2	47.0	50.6	73.0
Battery 1-3	48.1	47.2	72.2
Battery 1-4	48.3	47.6	71.2
Battery 2-1	44.3	47.8	71.0
Battery 2-2	43.6	46.6	71.0
Battery 2-3	47.0	44.5	70.0
Battery 2-4	48.3	45.5	69.8

With the failure of one of the TEC assemblies there is approximately a rise of 10ºC in battery temperatures with case 4 temperatures being slightly higher than case 3. One of the reasons for this difference could be due to the fact that in case 3, the functional TEC assembly is closer to the solar heater strips. With the failure of both the TEC the temperature rises by approximately 25ºC.

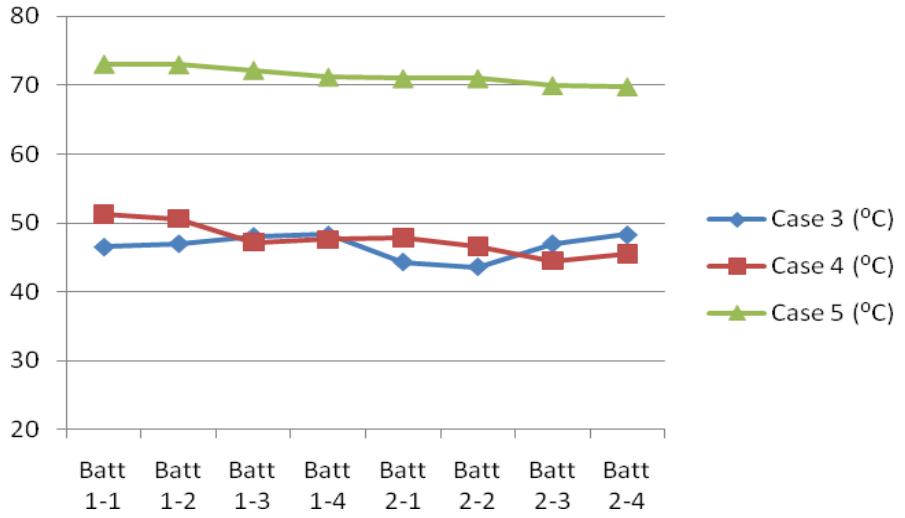

Figure 6.15 Comparison of Numerical results for various cases of TEC assembly failures

The impact of ambient air-flow on battery temperatures is studied through numerical analysis. The solution domain around the cabinet is modeled as an enclosure, with fixed air-flow provided in the x-direction i.e. normal to the front face of the cabinet as shown in Figure 6.16. This is done to mimic the effect of a wind tunnel. The enclosure is made sufficiently big enough so as to minimize the boundary effects on the air-flow around the cabinet. Battery temperatures for still ambient air and two free-stream velocities of 3 mph and 5 mph are recorded as Case 6, Case 7 and Case 8 respectively.

The results for this analysis are shown in Table 6.5. There is a decrease in battery compartment temperature with the increase in ambient air-flow velocity. This can be attributed to an improved overall heat transfer coefficient for the outer heat sink of the TEC air-air exchanger. There is a sudden drop in temperature of 3ºC when the air-flow changes from still air to air-flow at 3mph. Indicating that even a gentle wind blowing on the front face of the cabinet can improve the performance of the TEC air-air exchanger. Figure 6.17 and Figure 6.18 shows the vector plots for ambient air-flow of 3 mph and 5 mph respectively.

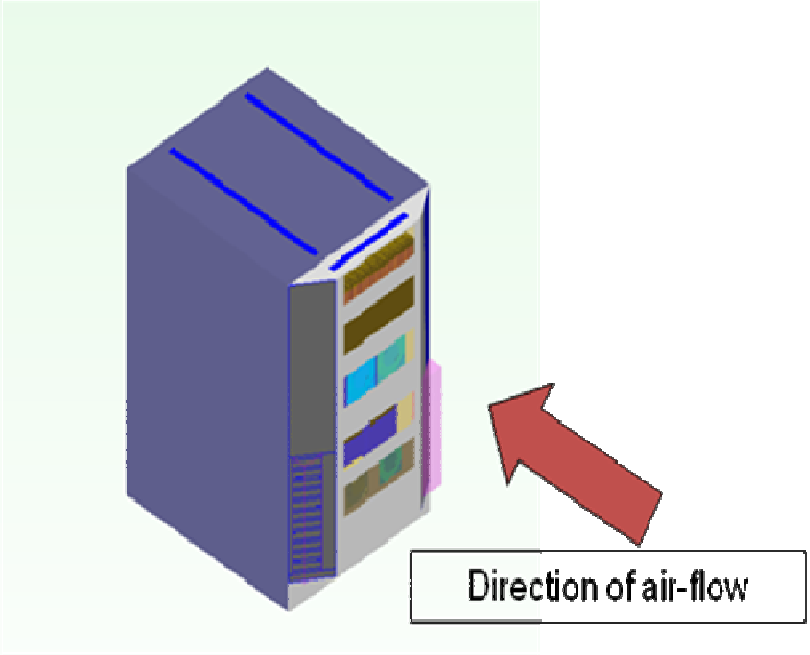

Figure 6.16 External view of the cabinet with direction of air-flow shown (isometric view)

Table 6.5 Comparison of Numerical Results for Still Air and Air-Flow at 3 mph and 5 mph

	Case 6 (ºC)	**Case 7 (ºC)**	**Case 8 (ºC)**
Battery 1-1	37.4	34.4	33.3
Battery 1-2	37.0	34.3	33.2
Battery 1-3	35.1	32.3	31.4
Battery 1-4	36.0	32.9	32.1
Battery 2-1	34.3	31.8	31.0
Battery 2-2	33.3	30.8	30.1
Battery 2-3	34.2	31.4	30.5
Battery 2-4	35.5	32.5	31.6

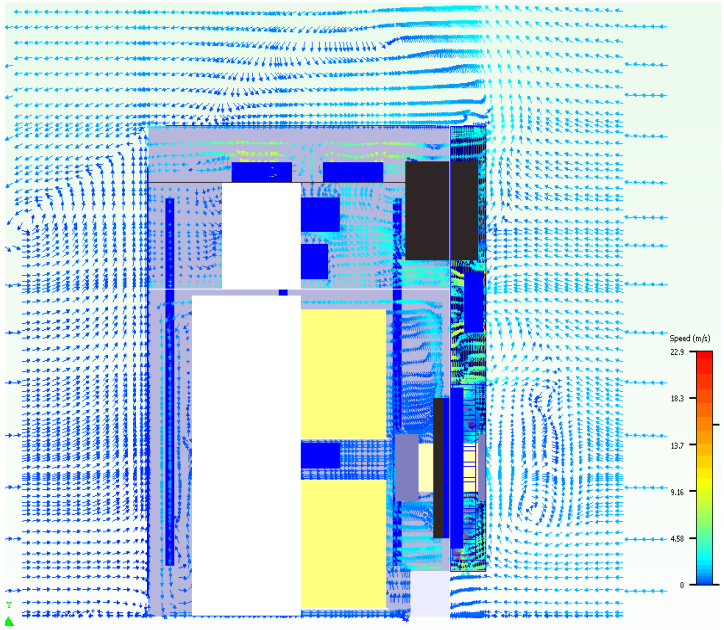

Figure 6.17 Vector plots for air-flow at 3 mph (side view)

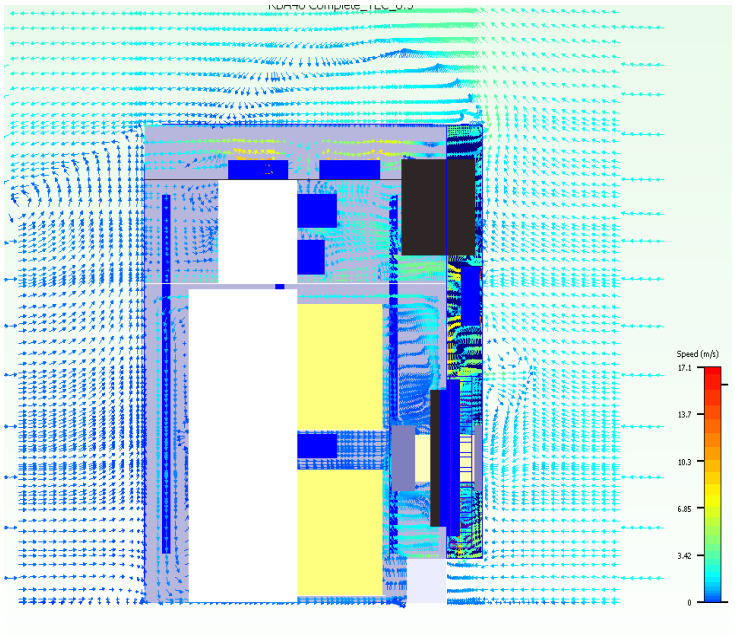

Figure 6.18 Vector plots for air-flow at 5mph (side view)

6.4 Conclusion

This study explains in detail, a novel method to numerically model a TEC air-air exchanger for system level cooling applications. This method uses readily available TEC macros, of a commercial CFD software, to model the assemblies in such a way as to mimic the functionality of these devices rather than the physical details of the thermoelectric devices.

Methods of enhancing the cooling effectiveness of the TEC assemblies by way of proper ducting to cut down on recirculation has also been discussed. Numerical analysis of the model with these enhancements has been compared with the numerical results of the model without them (base model). The results of both the scenarios compare well with the experimental results. Therefore, a reliable method to numerically model and test the TEC assemblies, without the need of proprietary information from the manufacturers, has been developed.

Further, the impact of failure of one or both of the TEC air-air exchangers on the battery temperatures and also the impact of external wind on the same has been discussed in this study.

APPENDIX A

METHOD TO COMPUTE THE PRESSURE DROP COEFFICIENTS FOR FILTERS IN FLOTHERM

The air-flow characteristics of a filter can be modeled using the volumetric resistance feature of Flotherm. This way the exact pressure drop vs. Flow rate behavior of the filter can be simulated in the model, thus giving us more accurate system resistance. This would in turn aid us in selecting the right fans to be used in cooling the system.

By using the advanced feature of volumetric resistance this capability could be incorporated.

The pressure drop for the volumetric resistance is given by

$$\Delta P = [A.\mu/2.l].v + [B.\mu.\rho/2.l].v^2 \qquad \text{(A1.1)}$$

ΔP - Pressure drop

v - velocity

μ- Dynamic viscosity

ρ-density

l - characteristic length = 1 m

Accurate values of both A and B coefficients needs to be computed and is given as an input in the advanced volumetric resistance dialog box. These coefficients are calculated from the system resistance curve obtained from experimental testing in a wind tunnel. The procedure is illustrated in an example given below:

Step 1 - The experimental results of Pressure and velocity for the filter are entered into the spread sheet.

Step 2 - The data points are plotted and a curve is fitted.

Step 3 - The fitted curve should be a second order polynomial and the intercept should be fixed to 0. This enables the equation to be compared with pressure.

Step 4 - Equating the coefficients of the above equation (A1.1) with the trend line equation obtained from the graph (shown in figure A1.1).

Equation of Trend line: $y = 602.68x^2 + 314.68x$

Table A.1 Static pressure drop and volumetric flow rate for the sample filter

Static Press. (in of H2O)	Flow Rate (CFM)	Flow rate(m^3/s)	Velocity(m/s)	Pressure (Pa)
0.05	81	0.03645	0.1458	12.445
0.09	85	0.03825	0.153	22.401
0.2	95	0.04275	0.171	49.78
0.35	115	0.05175	0.207	87.115
0.5	145	0.06525	0.261	124.45
0.72	185	0.08325	0.333	179.208
0.95	225	0.10125	0.405	236.455
1.2	260	0.117	0.468	298.68
1.5	300	0.135	0.54	373.35
1.8	350	0.1575	0.63	448.02
2.1	390	0.1755	0.702	522.69
2.4	440	0.198	0.792	597.36

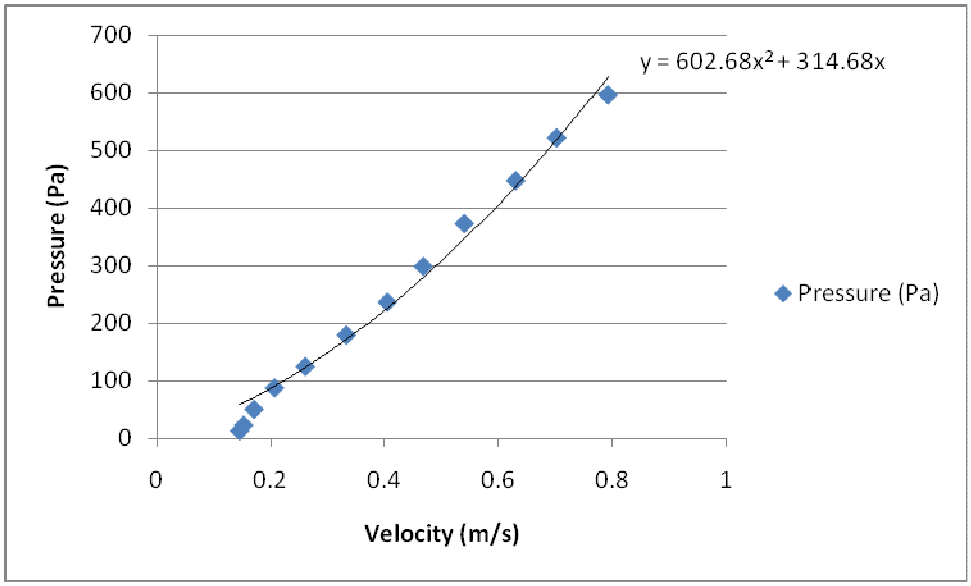

Figure A.1 Pressure vs. velocity profile for the sample filter

REFERENCES

[1] ASHRAE, "Thermal Guidelines for Data Processing Environments", Atlanta: American Society of Heating, Refrigeration and Air-Conditioning Engineers, Inc.,2004.

[2] Suhir, E. and Y.C. Lee, "Thermal, Mechanical and Environmental Durability Design Methodologies", Electronics Matreials Handbook, vol.1, ASM International, pp. 45-55,1989.

[3] Chanclou, P., Gosselin, S., Palacios, J.F., Alvarez, V.L., and Zouganeli, E., "Overview of the Optical Broadband Access Evolution: A Joint Article by Operators in the IST Network of Excellence e-Photon/One", IEEE com.mag., vol. 44, Issue 8, Aug. 2006, pp. 29 – 35.

[4] Charbonnier, B., Le Bras, H., Urvoas, P., N'Guyen, Q.T., Huchard, M. and Pizzinat A., "Upcoming Perspective and Future Challenges for ROF " IEEE International Topical Meeting on Microwave Photonics, 2007, pp. 21 – 23.

[5] Joshi, Y., Baelmans, M., Copeland, D., Lasance, C.J.M., Parry, J. and Rantala J., "Challenges in the Thermal Modeling of Electronics at the System Level: Summary of Panel Held at the Therminic 2000" Microelectronics Journal, Vol. 32, Issues 10-11, October-November 2001, pp. 797-800.

[6] Nie, Q. and Joshi, Y., "Multiscale Thermal Modeling Methodology for Thermoelectrically Cooled Electronic Cabinet" Numerical Heat Transfer, vol.2, pp. 371-406, 2000.

[7] NEMA. 2003. "Enclosures for Electrical Equipment (1000 Volts Maximum)`", NEMA Standards Publication 250-2003, Report by National Electrical Manufacturers Association, Rosslyn, VA.

[8] Telcordia Web site: http://www.telcordia.com/services/genericreq/digest/latest.html

[9] UL 50 - 2007. " UL Standard for Safety Enclosures for Electrical Equipment, Non-Environmental Considerations " UL 50, Underwriters Laboratory Inc., 2007

[10] Marongiu M. J., Helm R., Waiter K. and Kusha B., “Design and Development of a Passively cooled Remote Outdoor Cabinet”, Telecommunications Energy Conference, INTELEC. Twentieth International, 1998.

[11] Garcia M.P., Cosley M.R., and Marongiu M. J., "Experimental and computational studies on the Thermal Management of Electronics Enclosures using Natural Convection ", IMEC, Leuven, Belgium, 1995.

[12] Teertstra P.M., Yovanovich M.M., and Culham R., "Modeling of Natural Convection in Electronic Enclosures ", Proceedings of Inter Society Conference on Thermal Phenomena, pp. 140-149, 2004.

[13] Porebski W., and Ulfvengren R., “Passive cooling of small telecommunication enclosures, case study and practical approach,” in Proc. 20thInternational Telecommunications Energy Conference, INTELEC ’98, San Francisco, CA, Oct.4–8, 1998, pp. 562–567.

[14] Marongiu, M.J., Clarksean, R., Kusha, B. and Watwe, A., "Passive Thermal Management of Outdoor Enclosures Using PCM and Enhanced Natural Convection," 19th International Telecommunications Energy Conference, Melbourne, Australia, October 1997.

[15] Consentino P. A., "Thermal Management of Telecommunication Batteries using Phase Change Materials (PCM) Jacket " Power Conversion Products LLC., Crystal Lake, IL, USA, 2000.

[16] Choi, J., Jeon, J., and Kim, Y., Cooling performance of a hybrid refrigeration system designed for telecommunication equipment rooms, Applied Thermal Engineering 27, pp. 2026–2032, 2007.

[17] Maronjiu, M.,J., "Design of Compact Heat Exchanger for the Thermal Management of Battery Compartments of Outdoor Telecommunication Cabinets", TELESCON 97 proceedings, Budapest, Hungary, April 21-25, 1997.

[18] Muralidharan B., Iqbal Mariam F. A., Mulay V., Agonafer D., and Hendrix M., "Impact of Double Walled Telecommunication cabinet on Solar Load - Natural and Forced Convection" InterPACK 2009, San Francisco, CA, July 19-23, 2009.

[19] Muralidharan B., Iqbal Mariam F. A., Karajgikar S. and Agonafer D., " Energy Minimization based Fan Configuration for Double Walled Telecommunication Cabinet with Solar Load ", 26th SEMI-THERM Symposium, Santa Clara, CA, February 21-25, 2010.

[20] Linton, Ronald L.; Agonafer, Dereje, “Coarse and detailed CFD modeling of a finned heat sink,” IEEE Transactions on Components, Packaging, and Manufacturing Technology Part A, v 18, n 3, Sep, 1995, p 517-520.

[21] Narasimhan, S., Bar-Cohen, A., and Nair, R., "Thermal Compact Modeling of Parallel Plate Heat Sinks ", IEEE Transaction on Components and Packaging Technologies, vol. 26, pp. 147-157, 2003.

[22] Luo, Z., Ahn, H, and Nokali, M. A. E., "A Thermal Model for Insulated Gate Bipolar Transistor Module," IEEE Transactions on Power Electronics, vol.19, pp. 902-907, 2004.

[23] Trivedi A , Agonafer D , Sivanandan D , Hendrix M, and Saharpour A, “Compact modeling of Telecommunication cabinet”, ASME International Mechanical Engineering Congress and Exposition, Boston MA, October 31- November 6, 2008.

[24] McKay, J., "Predicting Transient Temperature Rise in Outdoor Cabinets Containing Telephone Equipment," Bellcore technical memorandum, TM-ARH-013463, January 26, 1989.

[25] Patankar, S.V., "Numerical Heat Transfer and Fluid Flow", Hemisphere, New York 1980.

[26] Flotherm Users Manual, Mentor Graphics Inc.

[27] Agonafer, D., Gan-Li, L., and Spalding, D. B., " The LVEL Turbulence Model For Conjugate Heat Transfer at Low Reynolds Numbers", EEP - Vol.18, Application of CAE/CAD Electronic Systems. ASME 1996.

[28] Dhinsa , K., Bailey, C., and Pericleous, K., " Low Reynolds Number Turbulence Models for Accurate Thermal Simulations of Electronic Components," Proc of the International Conference on Thermal and Mechanical Simulation and Experiments in Micro-Electronics and Micro- Systems, EuroSimE 2004.

[29] Launder, B. E., and Spalding, D. B., “The Numerical Computation of Turbulent Flows”, Appendix D of Computer Methods in Applied Mechanics and Engineering 3 (1974) 269-289. North-Holland Publishing Company.

[30] Woolfolk, A.," Specifying Filters for Forced Convection Cooling ", Electronics Cooling Magazine, Vol. 1, No. 2, October 1995, pp. 20-23.

[31] Turner, M., " All You Need to Know about Fans", Electronics Cooling Magazine, vol.2, no.2, pp. 10-13, May 1996.

[32] Ellison, G.N., " Fan Cooled Enclosure Analysis Using a First Order Method", Electronics Cooling Magazine, Vol. 1, No. 2, October 1995, pp. 16-19.

[33] Phan, H.N., Agonafer, D., “Thermoelectric Analysis Using Modified Graphical Method”, InterPack 2009, San Francisco, CA, July 2009.

[34] Godfrey, S.," An Introduction to Thermoelectric Coolers" Electronics Cooling Magazine, vol. 2, no. 3, pp. 30-33, Sept. 1996.

[35] Melcor website: http://www.melcor.com/tec.html

[36] Rowe, D. M.," CRC Handbook of Thermoelectrics", CRC Press, Inc., 1995.

[37] CommScope Integrated Solutions website:
http://www.commscope.com/eng/product/cabinets_enclosures/index.html

[38] Mentor Graphics website: www.mentor.com

[39] Nguyen D. and Kokko M., “Application of CFD Technique in Thermal Design of a Telecommunication Base Station”, 9th International Flotherm User Conference, Orlando, Fl, October 18-19, 2000.

[40] Cosley M R, Garcia M P, "Battery Thermal Management System" Telecommunications Energy Conference,2004. INTELEC 2004, Chicago, Ill, September 17-24, 2004

[41] Flotherm website: http://www.mentor.com/products/mechanical/flomerics.html

[42] Marongiu, M.J., (1995) “Some Issues In Experimental Testing And Methodologies In The Thermal Management Of Telecommunication Components, Systems And Enclosures,” to be presented at 17th International Telecommunication Energy Conference (INTELEC),, The Hague, Holland, Oct 29-Nov. 1, 1995

BIOGRAPHICAL INFORMATION

Feroz Ahamed completed his Bachelors of Technology in Mechanical Engineering from the University of Kerala, India. He completed his Master of Science degree in Mechanical Engineering in May 2010. He was part of the Electronics, MEMS, Nano-electronics Systems Packaging (EMNSPC) research team from January 2008. His research mainly deals with system level packaging for telecommunication and data center cabinets. His research work has been done primarily in collaboration with Commscope Solutions Inc., Richardson, Texas.